University of California
Santa Barbara

Elucidating the effects of nucleic acid aptamers on protein aggregation

A dissertation submitted in partial satisfaction
of the requirements for the degree

Doctor of Philosophy
in
Biochemistry & Molecular Biology

by

Claire Huynh Tran

Committee in charge:

Professor Irene Chen , Chair
Professor Frederick Dahlquist
Professor Songi Han
Professor Kevin Plaxco

December 2020

The dissertation of Claire Huynh Tran is approved.

Professor Frederick Dahlquist

Professor Songi Han

Professor Kevin Plaxco

Professor Irene Chen , Committee Chair

November 2020

Elucidating the effects of nucleic acid aptamers on protein aggregation

by

Claire Huynh Tran

I would like to dedicate my thesis to my family.

Acknowledgments

To my family, thank you for your endless support and constant love during my academic pursuits. Your inspiring words and encouragement have always pushed me to achieve my goals.

To my committee, thank you for your support and guidance. Thank you Dr. Irene Chen for encouraging me to explore various research avenues. As my mentor, you have taught me valuable research skills and confidence. Thank you Dr. Frederick Dahlquist, Dr. Songi Han, and Dr. Kevin Plaxco. As my committee, you have taught me to think critically and push my scientific limits.

To past and current Chen Lab members, thank you for all the time each one of you has spent listening to my scientific plans and supporting me through intellectual discussion. I am happy I was able to engage with the respectful and generous scientific minds of the Chen Lab.

To my friends, you have made this experience worthwhile. I will cherish the memories I have made with all the bright and kindhearted people I have met at UCSB.

Claire Huynh Tran Curriculum Vitae

Education

2020 Ph.D. in Biochemistry and Molecular Biology, University of California, Santa Barbara.

2015 B.S. in Bioengineering, University of California, Riverside.

Publications

2020 **Tran,C. H.**, Blanco, C., Buell, A., Chen, I. Modulation of α-synuclein aggregation *in vitro* by a DNA aptamer. in preparation.

2018 Lloyd, J., **Tran, C. H.**, Wadhwani, K., Cuba Samaniego, C., Subramanian, H. K., & Franco, E. (2018). Dynamic control of aptamer–ligand activity using strand displacement reactions. *ACS synthetic biology*, 7(1), 30-37.

2017 Li, H., Dauphin-Ducharme, P., Arroyo-Currás, N., **Tran, C. H.**, Vieira, P. A., Li, S., ... & Plaxco, K. W. (2017). A Biomimetic Phosphatidylcholine-Terminated Monolayer Greatly Improves the In Vivo Performance of Electrochemical Aptamer-Based Sensors. *Angewandte Chemie International Edition*, 56(26), 7492-7495.

2014 Mardanlou, V., **Tran, C. H.**, & Franco, E. (2014, December). Design of a molecular bistable system with RNA-mediated regulation. In 53rd IEEE Conference on Decision and Control (pp. 4605-4610). IEEE.

Awards

2020 UCSB Graduate Division Dissertation Fellowship

2016 Connie Frank Fellowship

Abstract

Elucidating the effects of nucleic acid aptamers on protein aggregation

by

Claire Huynh Tran

Protein aggregation is an important topic for human health and biotechnology, with consequences in areas ranging from neurodegenerative diseases to therapeutic protein production yields. With these concerns in mind, methods to modulate protein aggregation are therefore essential. One suggested method to reduce protein aggregation is the use of nucleic acid aptamers, i.e., single-stranded nucleic acids that have been selected to specifically bind to a target. Previous studies in some systems have demonstrated that aptamer binding to their protein target inhibit aggregation. However, the mechanisms by which aptamers might reduce aggregation have not been fully determined. In the studies described here, we investigated published aptamers that target α-synuclein and Green Fluorescent Protein (GFP) and their influence on protein aggregation. A kinetic and structural analyses were performed to assess the mechanistic effect of the selected aptamers on protein aggregation. An observation in each study indicated the presence of aptamers resulted in an increase of higher order intermediates (i.e., oligomers) in solution. The increase in oligomer population due to aptamers highlights a potential mechanism by which aptamers may modulate the aggregation properties of proteins. The modulatory effect of aptamers on protein aggregation can significantly impact biotechnology by proposing alternative methods to address disease and protein therapeutics.

Contents

Chapter 1

Introduction: Protein aggregation and aptamers

1.1 Proteins

Proteins are structurally organized polymers consisting of amino acids linked together. Due to environmental forces, the nascent chain of amino acids folds and forms known secondary structures, α-helices and β-sheets. Continued intramolecular interactions result in the formation of tertiary structures, which forms the intricate, individualized shapes of proteins. Once structurally settled, proteins begin to adapt and function within the cell performing cellular maintenance and output. Their functional abilities range from catalyzing many of biochemical reactions to trafficking molecules all throughout the cell. While proteins have natural functions, researchers have discovered additional and different tasks for proteins. For example, Green Fluorescent Protein (GFP), first discovered in Aequorea Victoria, has been engineered to be an efficient and ubiquitously used fluorescent marker. GFP's inherent 'light-up' fluorescent features lends well to its use in observing important cellular events when attached to proteins of interests[1, 2]. The versatility of proteins also makes them strong candidates for diagnostics and therapeutics.

An example of this is antibodies, which are proteins used in the immune system to effectively target pathogenic molecules[3]. Due to their efficient binding, antibodies have been enhanced to be used in a variety of diagnostic assays (e.g. ELISA) to detect for diseases biomarkers like α-synuclein aggregates[4], which are often observed in those with Parkinson's disease[5, 6, 7]. Therapeutically, antibodies are used to target pathogens, alerting the natural immune system to remove the marked molecule[4, 8]. With this and more, proteins serve as crucial fixtures to witness biology's mysteries and address pathological consequences.

1.2 Protein misfolding and aggregation

A major problem proteins face is aggregation. Normally, proteins are soluble biopolymers and require a specific structure to function appropriately. Molecular chaperones are used to regulate misfolded proteins. However, there are circumstances where proteins are exposed to harsh stressors (e.g., pH, genetic mutations, storage conditions), causing a loss of defined structure and leading to exposure of aggregation-prone sites 1[9, 10, 11, 12, 13]. Altered pH effects electrostatic interactions experienced on the surface of the protein, causing structural instability[9]. Various genetic mutations can cause a change in protein sequence which can result in the destabilization of its structure14. During storage, pharmaceutical protein can experience thermal fluctuations and formulation changes (i.e., change in buffer or concentration/dilution of stock protein), driving proteins to unfold[10, 11]. Once structurally vulnerable, these proteins can accumulate together, form intermediate structures, and finally develop into aggregates. Protein aggregates are characterized into two structural types: disordered and ordered[13, 14]. Disordered aggregates are amorphous in shape, meaning no defined structure to characterize them by. Ordered aggregates are commonly referred to as amyloid fibrils, which are described as an assembly of β-sheet structures organized into a rod-like shape. While the structures

of these aggregates may differ, they all have negative consequences in human health and biotechnology.

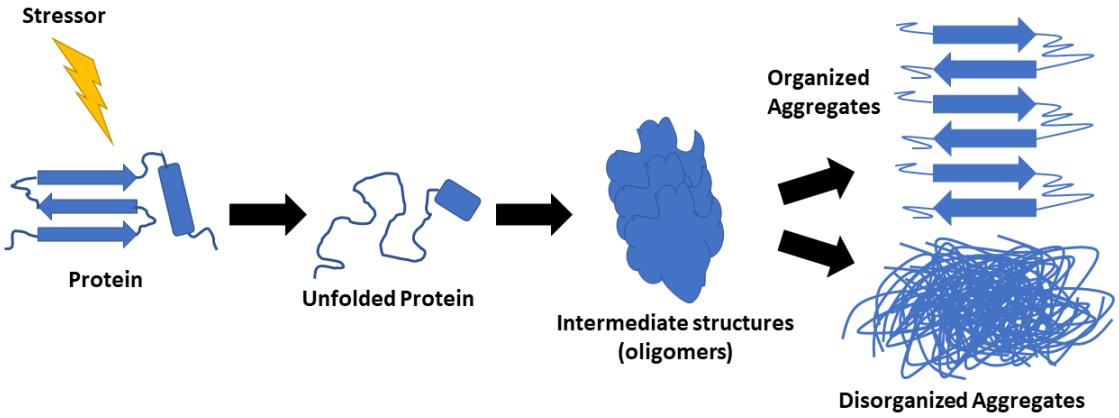

Figure 1: Scheme demonstrating the progression of protein aggregation from a stressor effecting protein structure to complete aggregate structures (i.e., organized aggregates v. disorganized aggregates). The mechanism displayed here is a generalized scheme; it can vary depending on proteins involved.

Protein aggregation is affiliated with many human diseases, especially neurodegenerative diseases. Several neurodegenerative conditions, including Alzheimer's and Parkinson's disease, are characterized by aggregating proteins forming insoluble, amyloid fibrils, (i.e., a cross β-sheet structure) or plaques[15, 16, 17]. Amyloid fibrils have demonstrated toxicity; however, recent work has posited small intermediates (i.e., oligomers) are the pathogens in these conditions[18, 19]. Whether it's the amyloid structure or its precursors, the outcomes remain detrimental. Biopharmaceuticals and technology are also negatively impacted by protein aggregation. Aggregation can cause problems in production yield of purified proteins and invoke unwanted immune responses (i.e., immunogenicity)[20]. Therapeutic proteins like insulin provoking an immune response is not beneficial for

the patient and can elicit further consequences. Given the serious concerns of protein aggregation, there is much interest in characterizing modulators for this process.

1.3 Current ways to mitigate consequences of protein aggregation

There are several ways in which mitigation of protein aggregation is achieved. However, it is important to know that there are disadvantages, especially the methods adopted in biotechnology.

With the use of molecular chaperones, the cell has regulated misfolded proteins and reduced aggregation. A popular example is GroEL, which is a chaperone present in bacteria that sequesters the unfolded region of a polypeptide away from external pressures[21]. Folding catalysts, like peptidylprolyl isomerases, are additional complexes used in the cell to accelerate folding of proteins[14]. While these complex systems generally help maintain stability of protein structure, the accumulation of protein aggregation is inevitable and overcomes the ability of the cell to appropriately respond resulting in diseases.

The approach for inhibiting protein aggregation in biotechnology can be combatted in two ways: modifying the protein and/or altering the surrounding environment. Modifying the sequence of a protein requires tedious step-wise mutations to ensure structural stability while maintaining function. The addition of chemical preservatives to adjust the protein's environment requires that the chemical species involved stabilize the protein, reduce aggregation, and do not hinder the proteins function. While both methods have been successful in reducing aggregation, they each have their drawbacks.

Modifying a protein's sequence through mutations has demonstrated promising results in inhibiting protein aggregation. Mutations performed on GFP to alter its net charge, exaggerating in either polar direction (+38, -40 v. -7; mutated v. standard) demonstrated solubility and structural resilience under thermal and chemical denaturation[22]. Although

successful, altering the protein's sequence can be cumbersome because each mutation increases the likelihood of structural and functional malformation. Additionally, this introduces concerns of immunogenicity, faltered function, and reduced viability. Changing the surrounding environment is another approach. One way is through the use of excipients which are inert molecules used to stabilize protein solutions[23, 14]. Sugars have been used as excipients to reduce protein aggregation. Sucrose stabilizes proteins by increasing the activation energy of the transition from a folded state to an unfolded state, making the unfolded state less favorable[24]. Small molecule additives have also shown promise in reducing denaturation and improving solubility. Small concentrations of polyamines in solution reduced the effects of lysosome aggregation caused by heat[25]. Altering the chemical environment of proteins is beneficial; however, the over addition of additives can saturate the environment and not address the consequences of all types of stressors. A study observing the ability of polyols to maintain solubility of protein under various stress conditions (thermal v. mechanical) concluded that no tested polyol universally maintained protein stability and solubility[26]. With these concerns, it would be highly advantageous to find a method or molecule that will be able to stabilize a protein under various harsh conditions while minimizing any immunogenic response.

1.4 Nucleic acid aptamers

Nucleic acid aptamers are postulated to be a potential option to address the concerns of protein aggregation. Aptamers, selected using *in vitro* evolution, are nucleic acid sequences that have maintained a secondary structure allowing them to effectively bind to a specific target[27, 28, 29]. This *in vitro* evolutionary approach 2begins with a randomized library of nucleic acid sequences, either RNA or DNA. The random library is incubated with the target of interest, ranging from small molecules to large proteins. The mixture is then processed to separate bound sequences from the unbound. Further

purification of the bound sequences is necessary to eliminate crude material and ensure quality nucleic acid sequences. Polymerase Chain Reaction (PCR) or Reverse Transcription Polymerase Chain Reaction (RT-PCR) is used to enrich the collected DNA or RNA, respectively. This enrichment process creates a new, refined pool of sequences, which undergoes the selection process until a small, viable number of sequences prevail (6-10 cycles on average). Further characterization is performed on the selected sequences to determine significant properties (e.g. binding affinity, secondary structure).

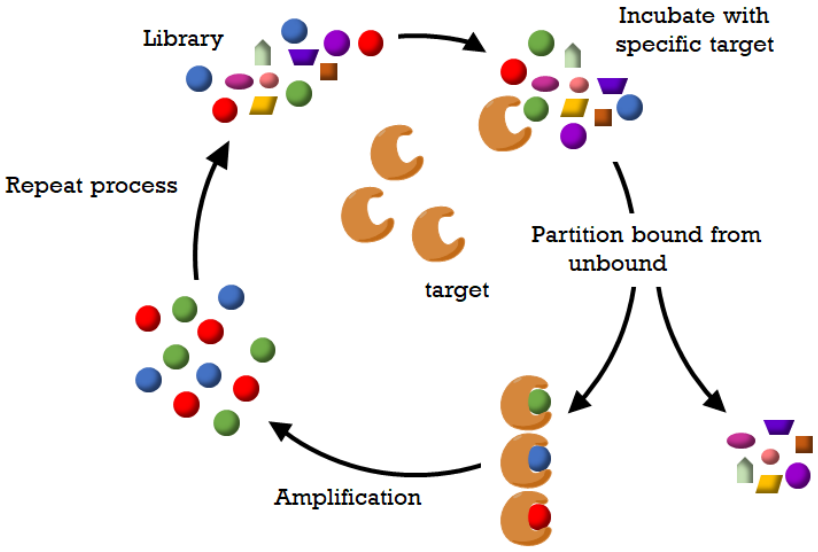

Figure 2: Schematic of *in vitro* evolution process.

The binding capabilities of aptamers make them a competitive alternative for diagnostics and therapeutics. Aptamers have several advantages over proteins, including their small size, immunogenicity, customizability, and stability. Aptamer-based diagnostic devices incorporate aptamer binding to a selected target and a signaling platform (e.g. colorimetric, fluorescence, electrochemical). There is a large sum of diagnostic assays that use aptamers to recognize various targets such as cocaine, thrombin, and proteins associated to Mycobacterium tuberculosis[30, 31, 32]. Additionally, aptamers are considered therapeutic agents. Pegaptnib Sodium is the first FDA approved aptamer therapeutic to treat neovascular age-related

macular degeneration (AMD) by inhibiting the binding of vascular endothelial growth factor (VEGF) to its receptors reducing the onset of neovascular AMD[33]. The versatility of aptamer application demonstrates the increasing functional benefit of this marvelous biomolecule.

1.5 Pervious work on nucleic acid aptamer mediated protein aggregation

Thus far studies have focused on the interaction between aptamers and proteins to determine any beneficial effects. One observation described was the stabilizing ability aptamers have on proteins. Under various stress conditions (e.g. thermal, mechanical and freeze-thaw), RNA aptamers selected stabilized tetanus toxoid, an inactivated form of tetanus toxin primarily used as therapy against tetanus[34]. RNA aptamers selected to bind to bovine insulin have stabilized the monomeric form and allowed the protein to retain its function[35]. Work on prion protein, showed a modified RNA aptamer inhibited the transition PrP^C to PrP^SC, the aggregation prone isoform connected to transmissible spongiform encephalopathies (TSEs)[36]. Additional to their stabilizing effect, aptamers also have been proposed as potential candidates to inhibit protein aggregation[37] and indeed there have been several reports of aptamers inhibiting protein aggregation[35, 38, 39, 40, 41]. The negative effects of mechanical induced aggregation on bovine insulin were reduced in the presence of RNA aptamers as shown through a decrease in solution turbidity/citeMalik2013. *In vitro* studies on amyloid β (Aβ) have demonstrated that RNA aptamers inhibit fibrillation of Aβ1-40, despite relatively low binding affinity[38]. Similar studies on tau protein showed that RNA aptamers against tau prolonged the oligomerization phase of tau[39]. These *in vitro* effects can influence the cellular setting as well. The aptamers against tau protein reduced the cytotoxic effects of tau overexpression, and also reduced the neurotoxicity of extracellular tau oligomers on primary cell culture neurons[39]. RNA aptamers selected against monomeric

segments of mutant huntingtin (51Q-mhtt & 103Q-mhtt) improved the solubility of mhtt in yeast cells and fixed endocytotic defects caused by aggregation of 103Q-htt[40]. Finally, peptide-mediated delivery of DNA aptamers selected against α-synuclein into cell lines overexpressing α-synuclein resulted in a reduction in toxicity, recovery of mitochondrial function, and improvements from cellular defects[41]. These studies have shown promising results for combining aptamers with proteins and the benefits on this interaction. Aptamers have the potential to be effective in resolving a severe biological problem, protein aggregation. This is an exciting development with significant implications in disease biology and biotechnology, requiring continued investigation.

Chapter 2

Permissions and Attributions

- The work in Chapter 2 and the Appendix for Chapter 2 is the result of a collaboration with Dr. Celia Blanco and Dr. Irene Chen. Reproduced in part with permission from Biochemistry, submitted for publication.
- The work in Chapter 3 and the Appendix for Chapter 3 are the result of a collaboration with Dr. Ranajay Saha, Thomas Nguyen and Dr. Irene Chen.

Chapter 3

The modulation of α-synuclein aggregation using DNA aptamers

3.1 Introduction

Intrinsically disordered proteins (IDPs) are of special interest for aptamer-based inhibition of aggregation, due to the connection between IDPs and neurodegenerative diseases. α-synuclein (SCNA, UniProtKB P37940) is a 14.4 kDa IDP expressed in the brain and is associated with multiple neurodegenerative diseases, collectively termed synucleinopathies. Like many IDPs, α-synuclein appears to be natively unfolded in solution, and pathological aggregation results in formation of β-sheet amyloid structures (amyloid fibrils). Although still under debate, α-synuclein oligomers are considered to be the likely toxic species. A previous line of work has demonstrated promising therapeutic effects of DNA aptamers having nanomolar affinity, selected against an immobilized GST fusion to α-synuclein, delivered to primary neurons[41] as well as in a mouse model of Parkinson's disease[42]. While a reduction of fibril formation was observed in vitro using these aptamers, the molecular mechanism of aptamer-induced inhibition was not studied further. In addition, an independent study reported the development of DNA aptamers selected to bind α-

synuclein oligomers17. These aptamers were selected to bind to α-synuclein oligomers under two conditions: a gel-shift assay in earlier rounds and a competitive dot-blot assay in later rounds. Some of these aptamers were further characterized to have dissociation constants in the nanomolar range, establishing high binding affinity. Based on these studies, we undertook an in vitro examination of the mechanism of aptamer-induced inhibition of α-synuclein aggregation.

The mechanisms by which aptamers inhibit protein aggregation are likely to vary depending on the specific system. For example, aptamers raised against monomers may act simply through stabilization and solubilization of the monomeric form[40], decreasing the driving force and/or rate of aggregation. Here, we focused on the DNA aptamers that had been selected to bind α-synuclein oligomers[43]. Reduction of oligomerization is of high interest since oligomers are increasingly thought to be the cytotoxic species. In principle, reduction of oligomerization could result from multiple possible mechanisms, such as binding to interfere with and slow the rate of on-pathway nucleation steps, or binding to induce creation of an intermediate form off of the aggregation pathway (an off-pathway intermediate). Our investigation suggests that one of the aptamers, T-SO508, inhibits aggregation through creation of an off-pathway oligomeric species, but not all DNA aptamers for α-synuclein oligomers have the same effect. The results broaden the understanding of possible molecular mechanisms underlying aptamer-induced inhibition of aggregation.

3.2 Results

3.2.1 Aptamer T-SO508 inhibits α-synuclein aggregation

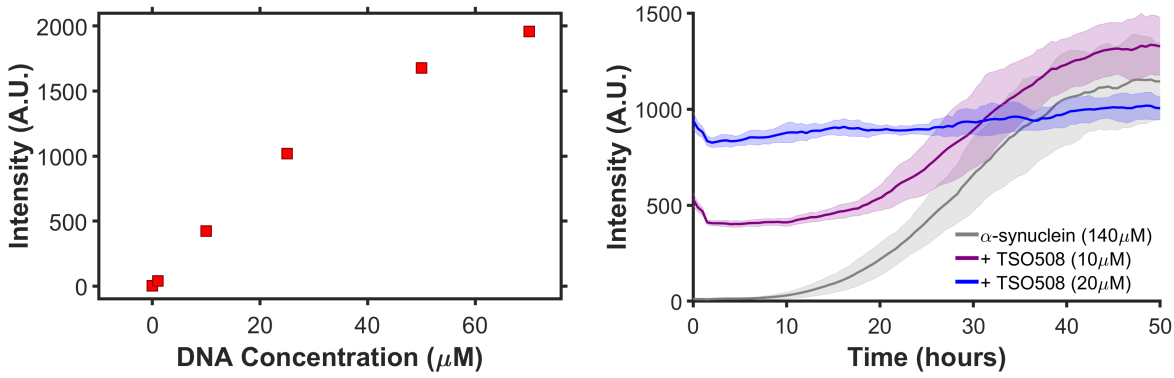

(a) (b)

Figure 1: α-synuclein aggregation in the presence and absence of T-SO508, followed by thioflavin T (ThT) fluorescence. (a) Dependence of fluorescence on T-SO508 aptamer concentration at 60μM ThT without α-synuclein. (b) α-synuclein (140 μM) aggregation in the presence of 60 μM ThT and 0 (gray), 10 (purple), or 20 μM (blue) T-SO508. Shaded area represents 1 standard deviation (n=3-5). The initial background fluorescence is consistent with the DNA concentration. A reduction in the sigmoidal kinetics was observed at higher [T-SO508] A.U. = Arbitrary Units

Aggregation of α-synuclein was assayed by thioflavin T (ThT) fluorescence. ThT is a cationic dye whose fluorescence increases upon interaction with protein fibrils, allowing kinetic monitoring of amyloid formation[44]. Aptamer T-SO508 was previously reported to bind to α-synuclein with a dissociation constant (KD) of 68 nM[43]. To probe the effect of T-SO508 on α-synuclein aggregation, T-SO508 was added in varying concentration to 140 μM α-synuclein. Aggregation was induced through agitation of glass beads in a 96-well plate at 37 C and monitored in a fluorescence plate reader.

In the absence of aptamer, α-synuclein aggregation was observed as a sigmoidal rise in fluorescence over approximately 2-3 days. We noted that the aptamer itself (without α-synuclein) caused increased ThT fluorescence, consistent with the known interaction

between ThT and DNA structures[45, 46]. ThT fluorescence increased linearly with the concentration of T-SO508 up to a T-SO508 concentration of roughly 30 μM (1a). The fluorescence of ThT in the presence of T-SO508 therefore could quantitatively account for an observed increase in the initial background fluorescence (time zero) of α-synuclein samples containing T-SO508 (1b). Little change in ThT fluorescence was observed for α-synuclein samples in the presence of 20 μM T-SO508 (0.14 equivalents), suggesting that this aptamer inhibited protein aggregation.

However, it was desirable to rule out the possibility that this finding was due to a greater affinity or irreversibility of ThT binding to aptamer that might render ThT insensitive to the presence of protein aggregates formed during the assay. To determine whether ThT would be able to detect newly formed aggregates in the presence of T-SO508, we added α-synuclein fibrils, prepared after incubation for 90 hours under aggregation conditions, to a solution of T-SO508 aptamer (20 μM) and ThT (60 μM). The fluorescence of the control sample without added fibrils was 656 $\pm$ 6 A.U. (arbitrary units), while the fluorescence of the sample containing the added fibrils was 736 $\pm$ 6 A.U. The fluorescence increase upon addition of fibrils indicates that the concentration of aptamer used in this experiment did not saturate the binding interactions of ThT, such that newly formed amyloid fibrils should still be detectable. These results support the use of these conditions (buffer, ThT and aptamer concentration) to monitor aggregation kinetics and fibril growth in the presence of T-SO508. Therefore, the lack of sigmoidal fluorescence increase observed for α-synuclein in the presence of 20 μM T-SO508 under aggregation conditions indeed indicates a lack of aggregation.

3.2.2 Aptamer T-SO508 prolongs the lag phase of α-synuclein

While qualitatively interesting, the results in the presence of high concentrations (20 μM or greater) of T-SO508 were difficult to interpret quantitatively since little or no

dynamics were observed. Therefore, we examined the effect of low, substoichiometric concentrations of T-SO508 on α-synuclein aggregation. Low concentrations of T-SO508 (¡10μM) did not affect the initial fluorescence substantially and allowed for observation of some kinetics of α-synuclein aggregation, at 140μM α-synuclein, using ThT (1b). We used two methods to quantify the effect of these low T-SO508 concentrations on aggregation kinetics: a model-independent, phenomenological analysis (MI) as well as fitting to the two-step Finke-Watsky model of aggregation (FW).

In the model-independent approach, the sigmoidal aggregation curve is characterized by a lag time and a growth rate. The lag time (t_{lag}) was defined by Shoffner et. al.[47] [Shoffner, 2016] as the time between the start of the experiment and the time of the intersection between the tangent drawn at the point of maximum growth rate and the average minimum fluorescence value (Sup. Figure 1). At 10 μM T-SO508 aptamer, tlag was increased significantly compared to no aptamer (2a). In MI analysis, the growth rate is measured as the slope of the tangent line at the highest rate of change, the position of which is determined by the maximum of the first derivative of the data set. No significant change was observed in growth rate when T-SO508 aptamer was added (2b).

The Finke-Watzky aggregation model[48, 49] is based on two elementary kinetic steps. The first step models conversion of the protein to an aggregation-prone state (i.e., nucleation), and the second step models autocatalytic conversion to the aggregated state (i.e., growth). Data are fit to this model with two parameters, namely the rate of nucleation (k_1) and the autocatalytic growth rate (k_2) (S11). Upon fitting the data, the presence of T-SO508 aptamer resulted in a substantial decrease in the nucleation rate (by 4-fold at 5 μM T-SO508 and 75-fold at 10 μM T-SO508) (2c), consistent with the observation of prolonged tlag in the MI analysis. A slight increase in the autocatalytic growth rate was also observed (2-fold at 10 μM T-SO508; 2d). The small size of this effect is consistent with the lack of statistically significant effect seen in MI analysis of

the growth rate.

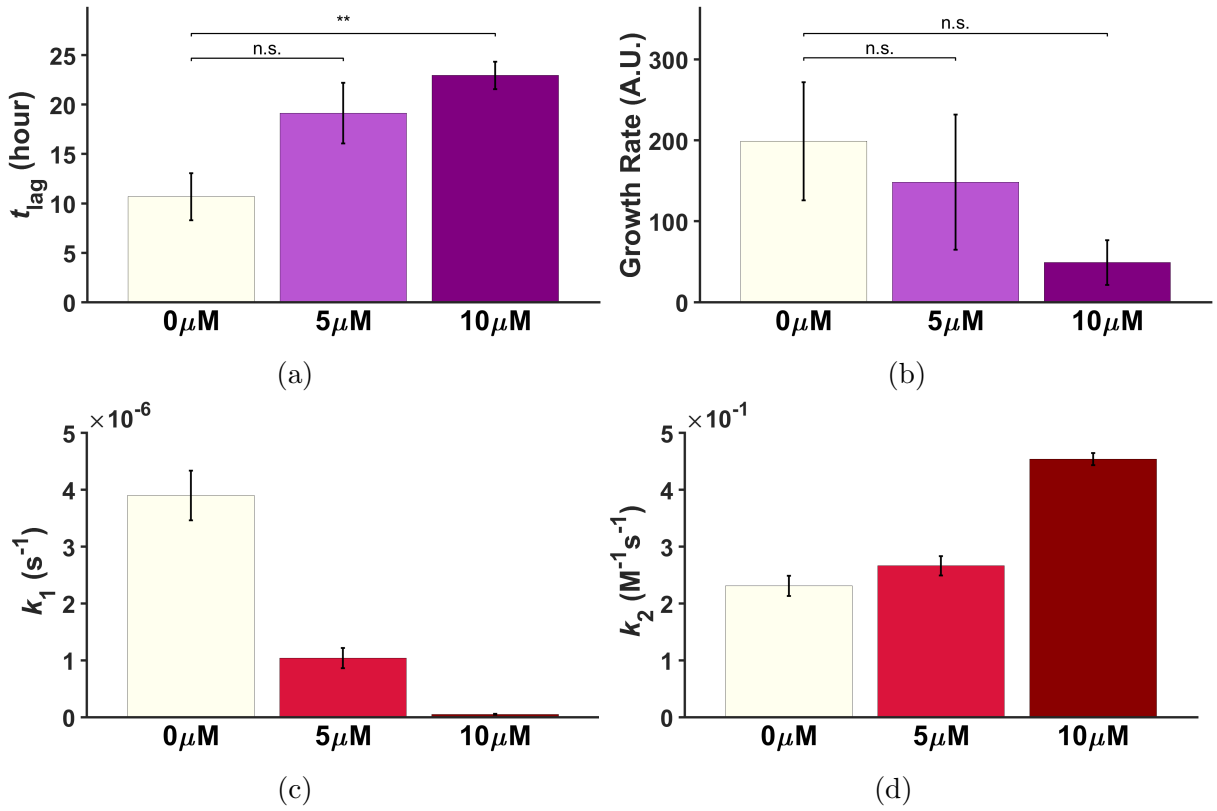

Figure 2: Effect of T-SO508 aptamer on aggregation kinetics. Samples contained 140μM α-synuclein, 60μM ThT, and 0, 5, or 10 μM T-SO508 (as indicated). Fluorescence traces were analyzed by MI analysis (a,b) or by the FW model (c,d). Error bars represent one standard error (n=6). MI analysis confirmed the slowed initial steps in the presence of T-SO508 (t_{lag} increased; 2a) and little or no effect on growth rate (2b). ** indicates p ¡ 0.01; n.s. = not significant. For FW analysis, the global fit of k_1 and k_2 demonstrated a pronounced decrease in nucleation rate (k_1; 2c) in the presence of T-SO508 aptamer and a slight increase in growth rate (k_s; 2d). Error bars for C and D represent the fitted parameter standard error for each condition.

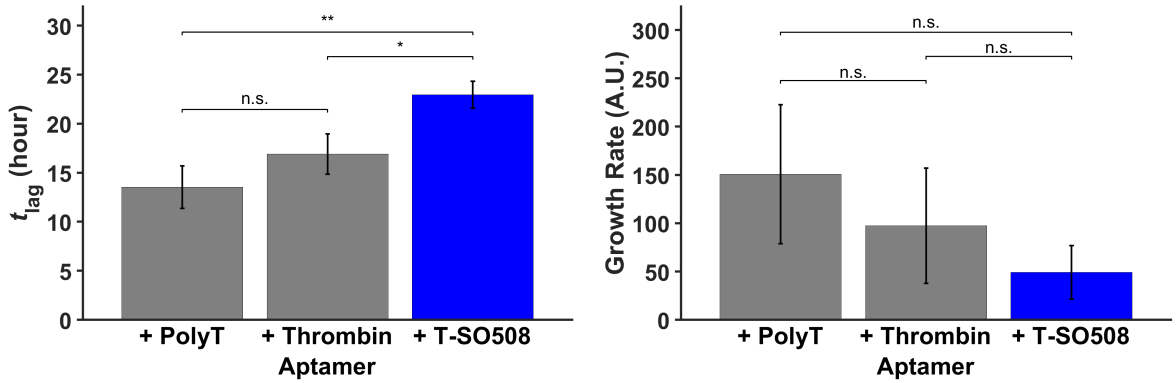

(a) (b)

Figure 3: Comparison of effects of T-SO508 aptamer and control DNA sequences. Samples contained 140μM α-synuclein, 60μM ThT, and 10 μM of poly-T sequence, thrombin aptamer, or T-SO508. Fluorescence traces were analyzed by MI analysis (a,b). a) T-SO508 prolonged t_{lag} significantly compared to control sequences. b) In contrast, growth rate shows no significant difference between T-SO508 and control sequences. Error bars represent one standard error (n=6; two-sample t-test: n.s.=not significant; *=p<0.05; **=p<0.01).

To further assess the statistical significance of the differences seen, an F-test was used[50] to determine whether the aggregation dynamics were different in the absence vs. presence of T-SO508 aptamer (5μM and 10μM). For the F-test, the different datasets (aggregation in the absence vs. presence of aptamer) were fitted together using the FW model, under the assumption that they follow the same dynamics, resulting in a single set of fitted parameters (k_1 and k_2). Then, the datasets were fitted separately, assuming the aptamer does affect kinetics, resulting in two independent sets of k_1 and k_2. Finally, the fittings were globally compared using an F-test (see methods), giving F-values of 136 and 812 for the T-SO508 aptamer concentrations of 5μM and 10μM, respectively ($p<10^{-5}$ in both cases), supporting the conclusion that T-SO508 aptamer significantly changes aggregation dynamics. In further analyses described below, the MI approach was preferred since the results were concordant between MI and FW analysis, and the appropriateness of the FW model for reactions containing aptamer was unknown.

To determine if the effects observed were specific to T-SO508, two control DNA sequences (a thrombin-binding DNA aptamer[51] and poly-T 24-mer sequence) were incubated with α-synuclein under the same conditions (3). As expected, the MI analysis showed that t_{lag} in the presence of T-SO508 was significantly longer than t_{lag} in the presence of the control sequences (3a). Although the underlying model was not appropriate, phenomenological fitting to the FW model supported the difference in lag phase (k_1) between T-SO508 compared to the control sequences (S12). These findings indicate that initial steps in the aggregation process appear to be inhibited specifically by T-SO508. Consistent with the results in the absence of aptamer, for the growth rate and k_2, both analyses showed little or no difference between T-SO508 and the control sequences (3b, S12).

3.2.3 Aptamer T-SO508 induces formation of small, aggregated structures

Although samples of α-synuclein incubated with high concentrations of T-SO508 were subject to high background when assessed by ThT fluorescence, such samples could instead be studied by atomic force microscopy (AFM) to understand any morphological changes of the particles. AFM was used to image the aggregates that developed in samples with or without excess T-SO508 (70 μM α-synuclein with or without 210 μM T-SO508). In the absence of T-SO508, α-synuclein aggregation produced fibrils, as expected, after 96 hours (4a). T-SO508 by itself was detectable by AFM as objects roughly 2.0 nm in height (4b,4d), consistent with a study which reported the visibility of similarly small single-stranded nucleic acids using AFM[52]. In contrast, in the presence of excess T-SO508 (molar ratio 3:1), α-synuclein subjected to aggregation conditions for 96 hours resulted in many roughly spherical, non-fibrillar structures (4c), in addition to some fibrils. The size of the spherical structures (7.4 nm in height) was significantly larger

than T-SO508 itself (1.9 nm in height) (S17), indicating that the structures observed were not simply deposited DNA. The observation of these structures suggested that T-SO508 induced formation of non-fibrillar aggregates with α-synuclein, which persisted for an extended period of time, i.e., beyond the point after which fibril formation of a sample lacking T-SO508 would have been complete.

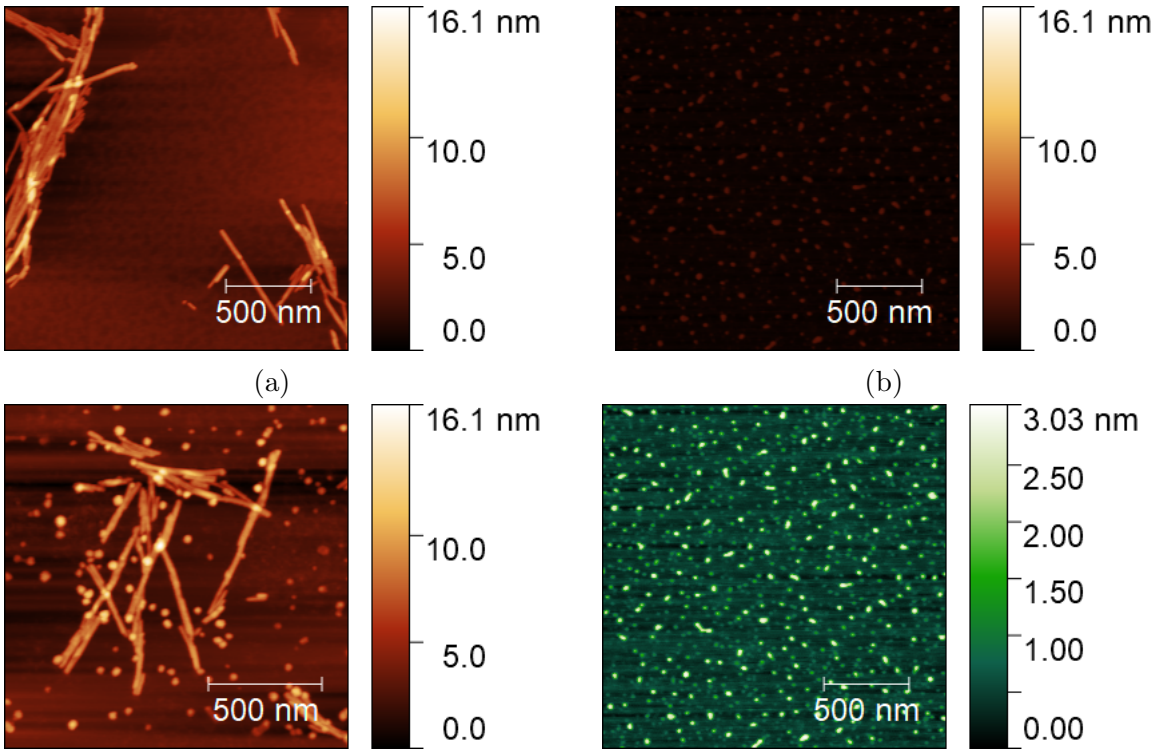

Figure 4: Observation of small aggregates induced by T-SO508 aptamer using atomic force microscopy. All samples were desalted, diluted (1:100) and deposited onto freshly cleaved mica. AFM height is shown by the heat map as indicated by the scale bars. (a) α-synuclein (70μM) after 96 hours of aggregation; (b) T-SO508 (210μM) aptamer deposited onto mica; (c) α-synuclein (70μM) with T-SO508 aptamer (210μM) after 96 hours of aggregation conditions; (d) same as (b) but with height scale adjusted for improved contrast.

3.2.4 Aggregates formed with T-SO508 do not seed fibril formation

Given that the presence of T-SO508 prompted formation of small aggregates, presumed to be oligomeric structures containing protein and DNA, we sought to determine whether these mixed aggregates were competent to act as seeds to form fibrils (i.e., accelerate aggregation kinetics). We prepared putative oligomers by 24-hour incubation of α-synuclein (70 μM) under aggregating conditions, in the presence or absence of T-SO508 (45 μM). This intermediate concentration of T-SO508 was chosen to avoid excessive unbound DNA while also being high enough to display inhibited aggregation kinetics. Fibrils were removed by centrifugation and excess DNA was degraded by DNase. The remainder was taken as 'seeds' for attempted nucleation of aggregation in fresh α-synuclein. 'Seeds' made in the presence of aptamer were compared to seeds made without aptamer. Seeds were also prepared in the presence of a control sequence (thrombin-binding aptamer) at 70 μM. Kinetics of seeded aggregation were followed by the ThT assay and analyzed by MI analysis, described above, to determine the effect on seeding behavior, as reflected in t_{lag}.

As expected, the addition of standard α-synuclein seeds (developed without DNA) shortened the tlag compared to an unseeded experiment. However, the lag time using 'seeds' developed in the presence of T-SO508 was significantly longer than that with seeds developed without DNA and seeds developed in the presence of the thrombin-binding aptamer (5). Indeed the lag time using 'seeds' developed with T-SO508 was similar to that of an unseeded experiment. These results indicate that T-SO508-induced structures do not promote aggregation, in contrast to standard α-synuclein oligomers. On the other hand, the presence of the thrombin-binding aptamer did not affect the seeds' ability to promote aggregation (t_{lag} similar with and without the thrombin-binding aptamer; (5)), indicating an effect specific to T-SO508. These results indicate that structures formed with T-SO508 are not competent for accelerating aggregation and are

biophysically distinct from pure α-synuclein seeds.

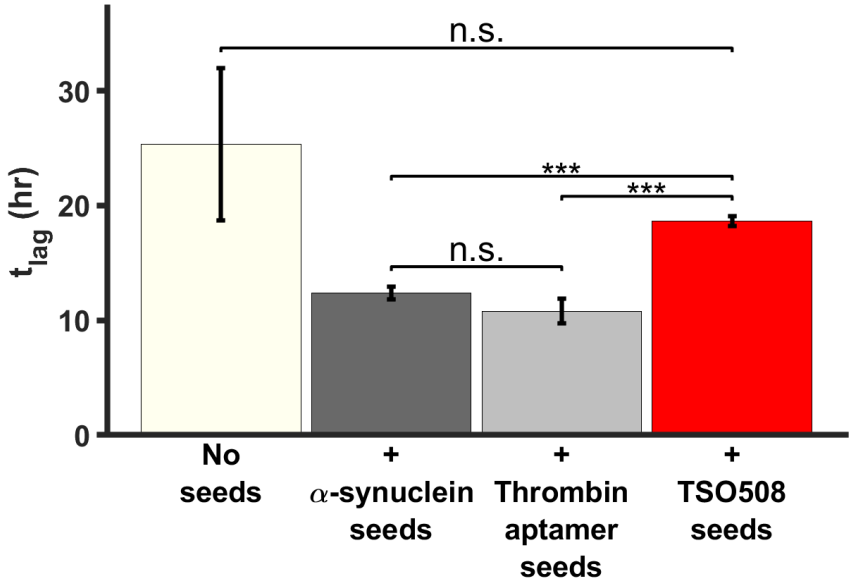

Figure 5: Oligomers formed in the presence of T-SO508 aptamer do not seed aggregation. Seeds were formed with 70 μM α-synuclein and one of the following: no DNA ('α-synuclein seeds'; dark gray), 70 μM thrombin aptamer ('thrombin seeds'; light gray), or 45 μM T-SO508 aptamer ('T-SO508 seeds'; red). Seeds were then added to a fresh solution of α-synuclein (140 μM). ThT fluorescence was used to monitor aggregation. Data were analyzed by the MI method. Seeds developed in the presence of T-SO508 do not shorten t_{lag} (no seeds vs. T-SO508 seeds), in contrast to seeds developed with the control DNA or no DNA. Error bars are one standard error (n=4; p-values for two-sample t-test are indicated: n.s. = not significant, *** = p<0.001

3.2.5 Lack of effect from a different α-synuclein-binding aptamer (T-SO530)

To determine whether the inhibitory effect of T-SO508 on α-synuclein aggregation was generalizable to other α-synuclein aptamers, we also studied the effect of aptamer T-SO530, which was previously discovered from the same selection and reported to bind α-synuclein oligomers with a similar affinity as T-SO508 (K_D of 68 nM for T-SO508 and K_D of 63 nM for T-SO530[43]). However, the presence of T-SO530 during α-synuclein aggregation did not exhibit the same prolongation of the tlag as the T-SO508 aptamer, as monitored by ThT fluorescence. There was no significant difference among the lag times observed in the presence of T-SO530 aptamer or control DNAs (thrombin-binding aptamer and poly-T) (6).

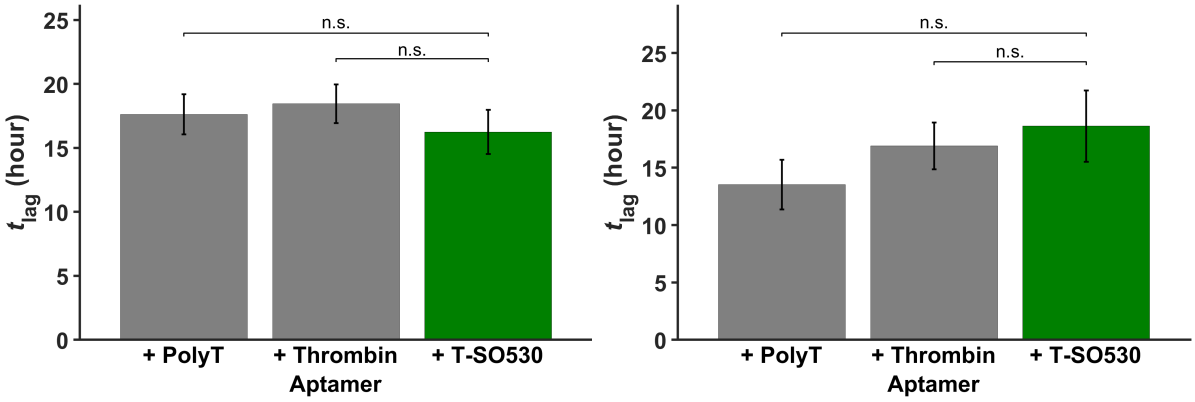

(a) (b)

Figure 6: T-SO530 aptamer does not prolong the lag phase of α-synuclein aggregation. All samples contained 140μM α-synuclein, 60μM ThT, and the DNA indicated at 5μM (a) or 10 μM (b). The fluorescence traces for each condition (n=6) were analyzed to obtain t_{lag} (MI method).

3.3 Discussion

In this study, we investigated the molecular mechanism behind the inhibitory effect of DNA aptamers on α-synuclein protein aggregation. We focused on T-SO508, which had been previously selected and demonstrated to bind α-synuclein oligomers with 60 nM affinity[43]. The assays here were performed in micromolar concentrations, so it can be assumed that nearly all of the aptamer was bound in these studies. The initial studies on aggregation kinetics, using established thioflavin T fluorescence assays, was highly suggestive of inhibition at the nucleation stage, in that even relatively low levels of aptamer (20 μM aptamer with 140 μM α-synuclein) appeared to result in extremely long lag times (longer than the assay time). However, these studies were also confounded by the known interaction of ThT binding to DNA[45, 46], which contributed high background fluorescence. While this did not prevent detection of fibrils (1b), it might complicate kinetic analysis. Thus, our analysis of kinetic studies was limited to low concentrations of DNA aptamer. The kinetic analysis showed little or no effect of the aptamer on the growth rate, which reflects the fibril elongation process. In contrast, low levels of aptamer significantly prolonged the lag phase, which reflects nucleation processes. The effect on nucleation processes is consistent with the original selection of the aptamer to target oligomeric species[43].

Two methods were used to analyze α-synuclein aggregation kinetics: a model-independent (MI) approach and the Finke-Watzky (FW) two-step aggregation model. The MI analysis allowed for a phenomenological characterization of an initial lag phase (t_{lag}) vs. the growth phase of aggregation, independent of a detailed mechanism. The FW model, while simple in having only two parameters, may not correctly represent the mechanism, as it does not treat the initial process of primary nucleation or the generation of intermediates[53, 54], and is not appropriate for experiments in which aggregation is seeded or inhibited by aptamers. However, more sophisticated reaction schemes that have been proposed

are intricate and involve a high number of parameters[53]. In cases for which both MI and FW analyses were applied, the results agreed, but we relied primarily on MI analysis here.

To further probe the effect of larger, stoichiometric amounts of aptamer at a structural level, we analyzed the reactions by atomic force microscopy. These results showed that T-SO508 caused formation of small, roughly round aggregates, not seen in α-synuclein alone and differing from the structures observed in T-SO508 alone. Interestingly, DNA can promote the formation of protein oligomers through DNA-oligomer networks[55], consistent with the observation that T-SO508 led to the development of α-synuclein oligomers. To establish whether these aggregates represented on-pathway intermediates of aggregation vs. off-pathway species, we attempted to seed fresh α-synuclein aggregation reactions with the aptamer-induced aggregates. We found that the aptamer-induced aggregates did not act functionally as nucleation seeds, indicating that the observed aggregates are off-pathway species. Furthermore, the observation that reactions treated with aptamer did not form effective 'seeds' suggests that they not only developed off-pathway aggregates but also failed to develop on-pathway oligomeric seeds.

Control experiments with DNA sequences that did not bind α-synuclein demonstrated that the inhibitory effects observed were specific to T-SO508. In addition, not all aptamers against α-synuclein inhibit aggregation, as another aptamer with similar dissociation constant isolated from the same selection, T-SO530, did not inhibit aggregation. Therefore, this work also highlights the fact that the mechanisms and effects of different aptamers may differ, so additional studies would be needed to probe the mechanism of other α-synuclein-binding aptamers, such as those used in cell culture and animal studies[41, 42].

Taken together, these results suggested that aptamer T-SO508 inhibits α-synuclein aggregation through formation of an off-pathway oligomeric species, which effectively shunts protein away from on-pathway species (7). To our knowledge, this mechanism

has not been previously reported for aptamer-induced inhibition of aggregation. It should be noted that the presence of this mechanism does not necessarily exclude other mechanisms, which may also be present but have lesser impact on the overall effect. Given the interest in using aptamers to control or modulate protein aggregation in therapeutic and/or biotechnological settings, the mechanisms underlying their effects warrant further investigation.

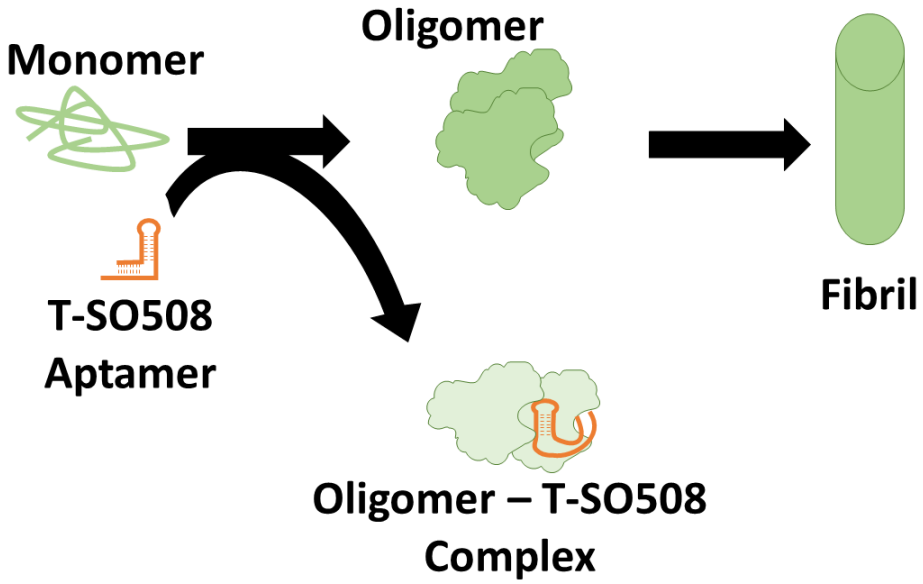

Figure 7: Scheme depicting inhibition of α-synuclein aggregation by T-SO508 aptamer mechanism.

3.4 Methods and Materials

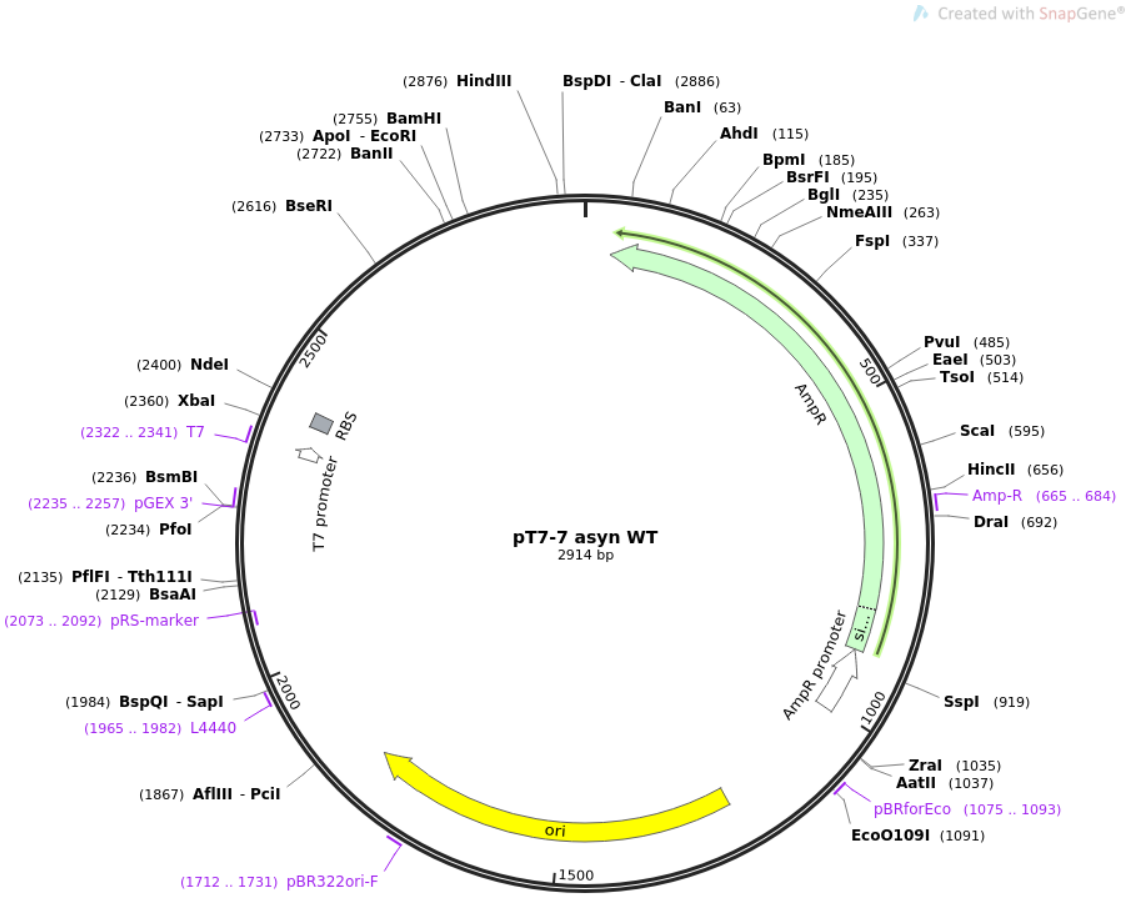

Figure 8: Plasmid map of α-synuclein contruct[56]

α-synuclein expression and purification: The pt7-7 construct containing α-synuclein (UniProtKB SNCA: P37840) was transformed into Escherichia coli BL21(DE3) competent cells (New England Biolabs). The construct was a gift from A. Buell, namely pT7-7 asyn WT (Addgene plasmid # 36046, gift of Hilal Lashuel;`http://n2t.net/addgene:36046`; RRID:Addgene_36046)[57]. α-synuclein expression was induced at an optical density (OD600) of 1-1.2 with 1 mM isopropyl-1-thio-β-D-galactopyranoside (IPTG; Sigma-Aldrich) at 37°C for 4-5 hours. Cells were harvested at 5,000xg for 15 minutes and resuspended in water. The cell resuspension was lysed at approximately 90C for

15 minutes. Lysate was centrifuged at 30,000xg for 40 minutes. The supernatant was collected and protein was precipitated using equal parts volume 4.5 M ammonium sulfate. The solution was centrifuged at 15,000xg for 30 minutes. The precipitate was re-suspended in 25mM Tris-HCl, pH 8.0 and dialyzed against 25mM Tris-HCl, pH 8.0. α-synuclein was purified using anion exchange chromatography and size exclusion chromatography. For anion exchange, the protein solution was loaded onto a HiTrap QFF column (GE Healthcare), which was equilibrated to 25mM Tris-HCl, pH 8.0. The elution gradient was set from 0-800 mM NaCl. Fractions containing α-synuclein were identified by SDS-PAGE, collected and concentrated using Amicon Ultra 15 Centrifugal Filter units (Millipore Sigma). The concentrated protein sample was then loaded on a HiPrep 16/60 Sephacryl S-200 HR column (GE Healthcare). Fractions containing α-synuclein were identified by SDS-PAGE and collected. Samples were flash-frozen in liquid nitrogen and stored in a -80C freezer for subsequent studies.

DNA Sequences: DNA sequences used here were based on previously published work[43, 51] (1). The sequences were synthesized and purchased from Bioneer.

Name	Sequence (5'—3')
T-SO508 aptamer	GCCTGTGGTGTTGGGGCGGGTGCG
T-SO530 aptamer	GGTGCGGCGGGACTAGTGGGTGTG
Thrombin aptamer	GGTTGGTGTGGTTGG
Poly-T sequence	TTTTTTTTTTTTTTTTTTTTTTT

Table 1: DNA sequences used in this study.

α-synuclein aggregation assays monitored by fluorescence: Aggregation of α-synuclein were performed in a Tecan M200 Pro instrument. Unless otherwise specified, experiments contained a buffer composition of 140 μM α-synuclein, 10 mM Tris-HCl (pH 7.4), 150 mM sodium chloride, and 5 mM potassium chloride. For fluorescence experiments, 60 μM Thioflavin T (excitation at 450 nm, emission at 485 nm) was added.

Experiments measuring the effect of aptamers used 0 - 10 μM aptamer. Mixtures (150μL) were pipetted into a 96-well plate (Corning) and placed into a plate reader (Tecan). A program was designed to continually agitate the samples by orbital shaking of 2 mm (280 rpm) using a 3 mm glass bead (Fisher Scientific) at 37C. Time zero was defined as the start of agitation. Fluorescence measurements were taken every 30 minutes.

Determination of lag time and growth rate of α-synuclein aggregation by model-independent (MI) analysis: We measured the lag phase as defined by Shoffner et. al.[47] A general scheme of the MI method is depicted in Supplemental Figure 1. Data was smoothed using a moving average to calculate the first derivative (Supp Fig 1B). A Gaussian was fit to the first derivative data set to determine the time of the peak value (tpeak; Supp Fig 1C). The time tpeak was located on the original data set and the slope of fluorescence increase (growth rate) was calculated. The intersect of the growth rate tangent at tpeak and the average minimum fluorescence value determined the length of lag phase, tlag (Sup Fig 1D).

Determination of nucleation and autocatalytic growth rates by Finke-Watzky (FW) model: The normalized fluorescence data was fitted to the Finke-Watzky two-step aggregation model[48, 49]: Where F(t) represents the polymeric form of the protein

$$F(t) = 1 - \frac{\frac{k_1}{k_2 \cdot A_0} + 1}{1 + \left(\frac{k_1}{k_2 \cdot A_0}\right) \cdot exp\left((k_1 + k_2 \cdot A_0) \cdot t\right)}$$

aggregate and k_1 and k_2 correspond to the average rate constants for nucleation and growth. A_0 is the initial concentration of monomeric form of the protein ($A_0 = 140\mu$M). Fittings were performed using Origin[58]. Datasets were normalized using the average of the first and last 10 points as minimum and maximum values. Datasets corresponding

to the same experiment (e.g. triplicates or sextuplicates) were merged and treated as a single curve. Errors in the fitted parameters correspond to the fitting standard error.
We performed three paired F-tests to compare aggregation dynamics in the absence and presence of aptamer T-SO508 aptamer at three different concentrations. The null hypothesis is that one curve fits all the data points (i.e. both datasets) and the observed difference is purely due to chance. We fitted a single curve to all the data from both datasets (i.e. with and without aptamer) and obtained one estimate for each of the two parameters in the model (k_1, k_2). The alternative hypothesis is that the curves are distinct, and hence, are ruled by different dynamics. The residual sum of squares and degrees of freedom for the combined set are denoted as SSR_{comb} and df_{comb}. To fit the alternative hypothesis, we fit each dataset separately to obtain two distinct curves with two different sets of parameters (k_1, k_2) for each data set (i.e. in the absence and presence of T-SO508 aptamer). The residual sum of squares and degrees of freedom for each pair of independent fits is RSS_1, RSS_2, df_1, df_2. The F value is then calculated as:

$$F = \frac{(SSR_{comb} - SSR_{sep})/(df_{comb} - df_{sep})}{SSR_{sep}/df_{sep}}$$

where SSR_{sep}=RSS_1+$RSS2$ and df_{sep}=df_1+df_2.

Seeding of aggregation: Fresh, filtered α-synuclein (70μM) was treated using the aggregation assay conditions described above. Reactions either contained: no DNA, T-SO508 (45 μM), or thrombin-binding aptamer (70 μM). After 24 hours of agitation, samples were collected and centrifuged for 30 minutes at 16,000 rcf at 4°C to precipitate out amyloid fibrils. The supernatant (seed-containing; presumed oligomers and monomers) was collected and 2-3 μl Salt-Activated Nuclease (SAN; Sigma Aldrich) was added. The mixtures were incubated at 25 °C for 3 hours for digestion of DNA. 10% of this seed mixture was added to 150 μL of aggregation reaction solution, containing fresh, filtered

α-synuclein (70 μM), buffer, and ThT. Samples were monitored using ThT fluorescence, as described above.

Atomic Force Microscopy experiments: Samples were imaged on an Asylum MFP-3D Standard System (Asylum Research, Santa Barbara, CA). Prior to imaging, samples were prepared by desalting reaction mixtures using a Zeba Spin Desalting Column, 7k MWCO (Thermo Scientific). Desalted samples were deposited onto a cleaved mica surface. Imaging was done in AC mode with FORTA probes (AppNano, Santa Clara, CA). Image processing and analysis was performed using Gwyiddion (http://gwyddion.net/).

Chapter 4

RNA aptamer stabilize Enhanced Green Fluorescent Protein oligomers

4.1 Introduction

The origins of Green Fluorescent Protein (GFP) began with a report of green fluorescence emitting from *Aequorea Victoria* when exposed to ultraviolet light[59]. Further work determined that GFP was the responsible for the fluorescence emitting from *Aequorea Victoria*. GFP has a molecular weight of 26.8 kDa and is composed of 238 amino acids that form 11 secondary structure β-sheets, further organized in a manner physically reminiscent of a barrel (Figure 1)[1]. In 1994, GFP was expressed in *E. coli* and *C. elegans*, beginning to demonstrate the special potential of this fluorescing protein[60]. Now, GFP and GFP mutants (e.g., Enhanced, Emerald, etc.) are attached to targets of interest, allowing for the observation of cellular events and mechanisms (e.g., gene expression, protein localization). The expanding use of GFP, establishes the importance of maintaining its stability and function.

Unfortunately, like many proteins, GFP is susceptible to aggregation[61, 62]. In

bacteria, GFP aggregates to form inclusion bodies, resulting in a loss of available, active protein[61]. Interestingly, GFP folds differently in bacteria and mammalian cells, illustrating a potential limitation for its use as a universal marker protein[63]. To address the concern of aggregation, GFP has been previously mutated to improve folding, fluorescence and reduce aggregation sensitivity. Unfortunately, mutations do not have an additive effect on GFP stability and function[1], reinforcing the importance of seeking alternative modulators for aggregation.

In this study, we explored the modulation effect of a reported RNA aptamer, AP3-1. This 83 nucleotide long RNA aptamer was selected to target GFP and similar fluorescent protein variants (5'-GGGAG CACGA UGGCG UGGCG AAUUG GGUGG GGAAA GUCCU UAAAA GAGGG CCACC ACAGA AGCAA UGGGC UUCUG GACUC GGU-3')[64]. We studied the effect of this RNA aptamer on Enhanced GFP (EGFP) aggregation to expand our understanding of how aptamers effect the mechanism of protein aggregation. A prior unpublished study in our lab on the effect of AP3-1 on Emerald GFP (EmGFP) suggested that AP3-1 may inhibit EmGFP aggregation [unpublished data, T. Nguyen]. To extend this work, we began an investigation of the mechanism behind AP3-1 inhibition of GFP. While the previous work was conducted on EmGFP, we studied the effect of AP3-1 on a different GFP mutant, namely Enhanced GFP (EGFP). EGFP has fewer mutations than EmGFP, resulting in increased susceptibility to aggregation[1], especially at low pH and high protein concentrations[65, 66]. Because aggregation of EGFP is more pronounced than EmGFP, and the AP3-1 aptamer had been already shown to bind EGFP in published work, we focused our studies on EGFP. We induced EGFP aggregation using three different methods and conducted static light scattering (SLS) measurements to determine the effect of AP3-1. Our study showed that light scattering increased when EGFP was aggregated in the presence of AP3-1, and the results suggest that AP3-1 increases formation of larger, but soluble, structures. A mechanistic

study on DNA aptamers and α-synuclein aggregation had suggested that an α-synuclein aptamer modulates protein aggregation by forming off-pathway oligomers [Tran et. al. in preparation]. These results build upon the concept that aptamers can modulate protein aggregation through different mechanisms and should be further examined for potential use in therapeutics.

4.2 Results

4.2.1 Confirming binding of AP3-1 to EGFP

As mentioned earlier, previous work in our lab focused on the discovery of the phenomenon that an RNA aptamer, AP3-1, inhibited Emerald GFP (EmGFP) aggregation [unpublished data, T. Nguyen, 2018]. We continued to elaborate on this phenomenon by using a different GFP construct, Enhanced GFP (EGFP), for the reasons mentioned above.

Prior to aggregation studies, it was important to confirm binding of AP3-1 aptamer to EGFP in our laboratory. We used two techniques to establish AP3-1 binding to EGFP: fluorescence and absorbance measurements. Previous fluorescence characterization of the AP3-1-EGFP complex demonstrated that EGFP fluorescence decreased upon binding of AP3-1[64]. Samples were prepared, for fluorescence measurements, with constant concentration of EGFP (25 nM) and varying AP3-1 concentrations (0-250 nM). Each sample was excited at 460 nm and an emission scan from 490-600 nm was collected for comparison. An observed decrease in EGFP fluorescence was revealed as AP3-1 concentration increased (1a). The declining fluorescence of EGFP correlated to successful binding of AP3-1 aptamer to EGFP and supported previously described AP3-1 properties[64]. Additionally to support the fluorescence analysis, an absorbance scan was performed to determine AP3-1 binding to EGFP. Shui et. al. described an absorbance spectrum in which the AP3-1-EGFP complex elicited an increase at 395 nm and decrease at 475 nm in comparison to EGFP only. An absorbance scan of AP3-1-EGFP (5μM:200nM) solution was measured and a similar trend, described above, was observed (1b). Fluorescence and absorbance measurements reinforced the characterization of AP3-1 binding to EGFP, supporting our use of AP3-1 to study this aptamer's effect on EGFP aggregation.

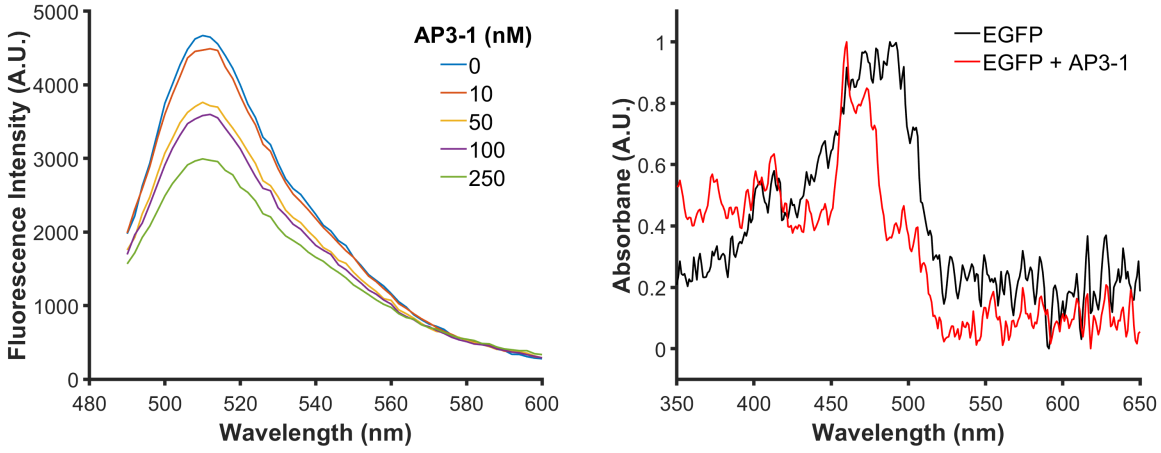

(a) (b)

Figure 1: AP3-1 binding to EGFP confirmed through fluorescence and absorbance measurements. a) Fluorescence measurements (ex: 460nm ;em: 490-600nm) were performed at varying concentrations of AP3-1 (0-250nM). b) Absorbance scans (350-650nm) were performed on two sample conditions. One set contained EGFP only at a concentration of 200nM, while the other sample set had EGFP (200nM) and AP3-1 (5μM).

4.2.2 Confirming aggregation techniques for EGFP

We explored two ways to aggregate EGFP, chemical aggregation and mechanical agitation. These methods simulate common stressors during the manufacturing and storage conditions of proteins. To confirm the presence of aggregates, we performed static light scattering (SLS) measurements. Light intensity values were collected from the SLS measurements, which correlate to the presence of structures in solution (e.g., higher light intensity values represent large/more structures in solution). These values were then compared and used to determine effectiveness of aggregation methods.

Chemical aggregation was induced by 2,2,2-trifluoroethanol (TFE), a common cosolvent used to form aggregates[67]. The addition of TFE (40% w/v) to EGFP (5μM) caused an increase in light scattering intensity, establishing the presence of higher ordered structures (2a). The mechanical agitation method was produced by shaking the samples in the

presence of glass beads. This mode of aggregation alters the air-water interface causing proteins to react and expose previously hidden sites, analogous to the harsh environment therapeutic proteins experience[68, 69]. A similar increase in light intensity was observed in samples with EGFP after mechanical shaking (2b). TFE and mechanical agitation were successful methods of aggregation.

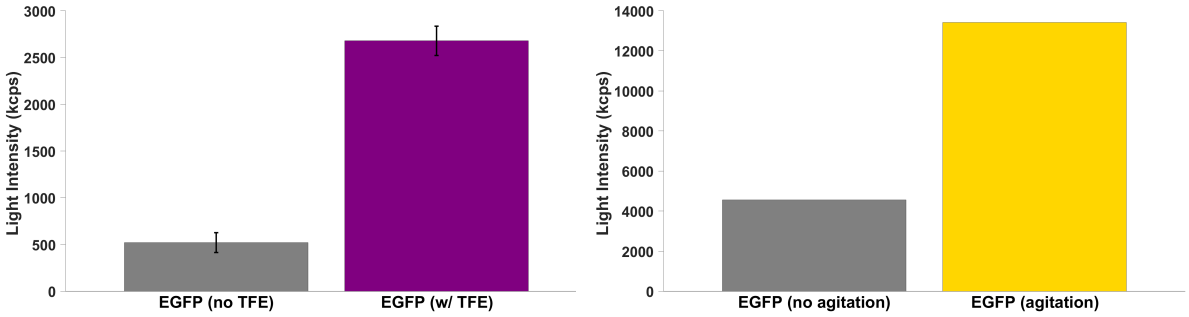

(a) (b)

Figure 2: Confirming selected methods result in protein aggregation. Static light scattering technique was performed on samples that experienced aggregation, chemically induced or mechanical agitation, and samples that did not undergo aggregation methods. a) Comparison between EGFP exposed to TFE and EGFP only, no TFE. The increased light intensity in samples exposed to TFE correlate to an increase in aggregates present. b) Mechanical agitation was performed on EGFP using glass beads and shaking. Samples that were not agitated had lower values of light intensity than agitated samples,alluding to the presense of aggregates by agitation.

4.2.3 Determining the effect of AP3-1 on EGFP aggregation

We tested the effect of AP3-1 on EGFP aggregation using three methods of aggregation discussed above: chemical, agitation and lyophilization and agitation. The drastic solution property changes involved in lyophilization (i.e. flash freezing the protein solution followed by removal of ice) can result in protein aggregation[70]. Pairing lyophilization with agitation, which was confirmed to cause aggregates (2), provided an additional comparison to investigate whether AP3-1 has a universal effect on EGFP aggregation.

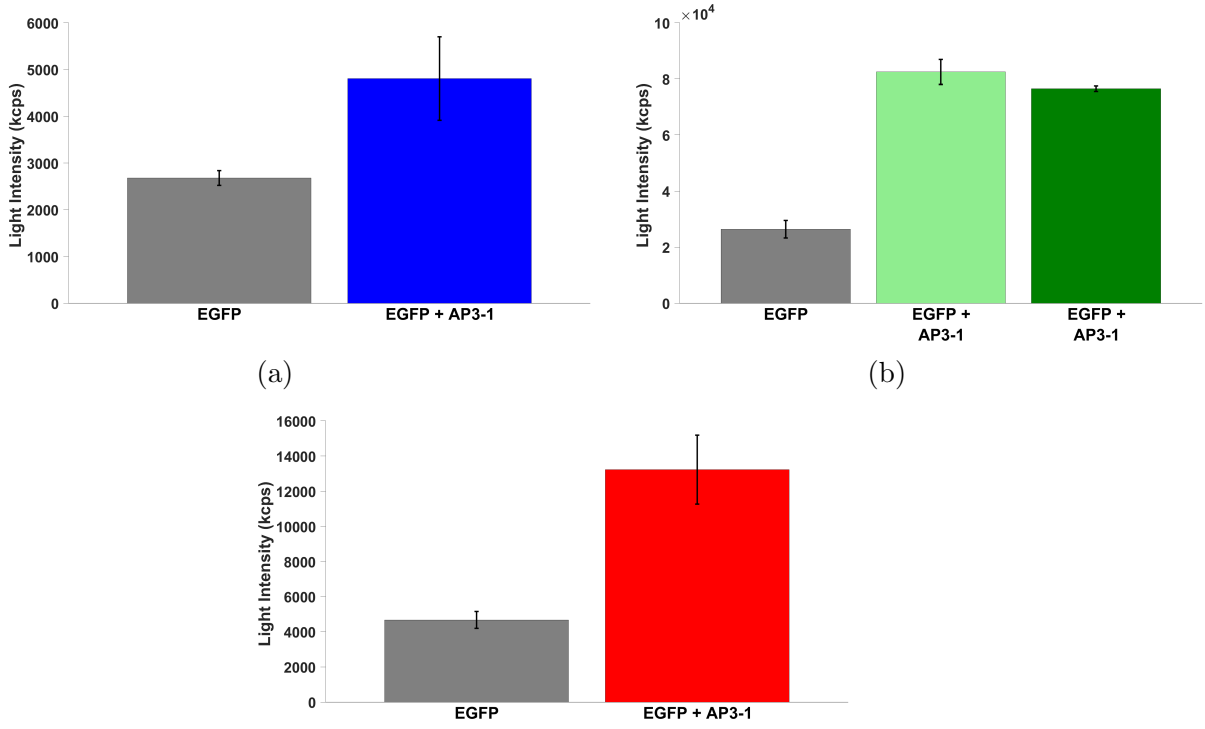

Figure 3: Changes in light intensity upon the addtion of AP3-1 in various induced aggregation systems. a) Chemically induced aggregation by TFE resulted in a difference between EGFP (5μM) and EGFP+AP3-1 (5μM:7.2μM) samples. b) Mechanical agitation invoked by glass beads and shaking resulted in an increase in light intensity in samples containing EGFP (1μM) and AP3-1(2μM or 4μM) unlike EGFP only. The light green bar indicates a solution composition of EGFP and AP3-1, 1:2 molar ration. The green bar represents a solution of EGFP and AP3-1 1:4 molar ratio. c) An increase in light intensity was observed in lyophilized samples containing EGFP(500nm) and AP3-1(1muM) than EGFP. Error bars are 1 standard error.

For lyophilization, samples were freeze-dried and resuspended in a buffer (137 mM NaCl, 2.7 mM KCl and 10 mM phosphate, 5 mM $MgCl_2$) at a low volume, followed by agitation. Irrespective of the aggregation methods, samples containing AP3-1 resulted in a 2-3 fold increase in light intensity compared to the EGFP only samples(3). Varying the concentration of AP3-1 by 2 to 4 times more than EGFP did not affect the result, indicating that the observed effect is concentration independent (3b). The static light

scattering method suggested an increased number of large aggregate structures being present in the solution with AP3-1, which remains consistent with varying methods of aggregation.

4.2.4 AP3-1 maintains soluble high-order structures

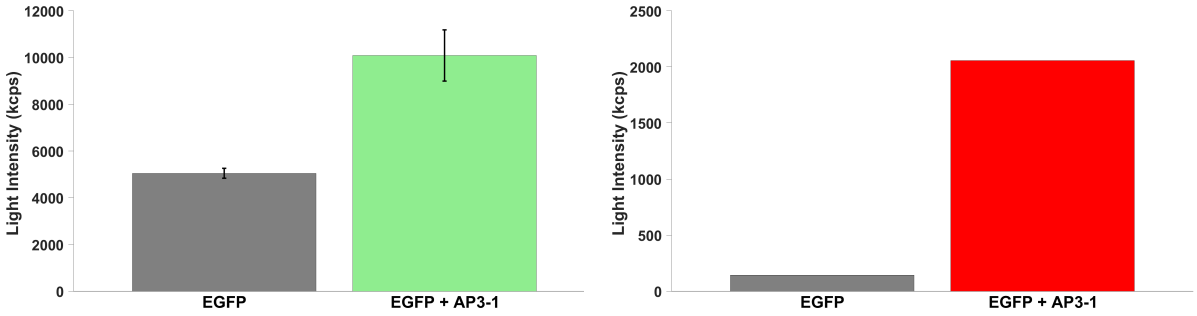

(a) (b)

Figure 4: SLS data confirming the presence of soluble species in samples containing AP3-1. EGFP-AP3-1 samples were at a molar ratio of 1:2. a) EGFP-AP3-1 (1μM:2uM) samples maintained an increase number of soluble structures than EGFP samples and shown through SLS data. b) Lyophilized samples of EGFP and EGFP-AP3-1 (500nM:1μM;) collected different light intensity values establishing the presense of more soluble structures present in EGFP-AP3-1 samples.

An increase in light intensity in samples containing AP3-1, insinuated the presence of many high-order structures in solution. We set out further characterization of these structures, by determining whether these structures were soluble or insoluble. We devised a protocol to sediment insoluble aggregates via centrifugation and collect soluble fractions in the supernatant. SLS data showed a maintained increase in light intensity of the supernatant from samples containing EGFP and AP3-1 (molar ratio 1:2) (4). Under agitation (4a) and lyophilization-agitation (4b) conditions, samples containing AP3-1 measured larger light intensity values than EGFP alone. These results suggested that mixture of EGFP and AP3-1 contained more soluble structures than the controls (EGFP only). The increased light intensity of EGFP-AP3-1 samples in Figure 3 can

be attributed to an increased population of soluble structures and not due to insoluble aggregates. Overall, the data suggested that AP3-1 maintains increased proportion of soluble structures in the protein solution induced for aggregation.

4.3 Discussion

This study focused on elucidating the impact of AP3-1, a RNA aptamer, on EGFP aggregation. We tested various methods of aggregation (chemical induction, mechanical agitation, and lyophilization) and compared the effect of AP3-1 on EGFP at equimolar concentrations or excess AP3-1 concentrations to ensure binding to EGFP. Prior to aggregation studies, it was imperative to confirm AP3-1 binding to EGFP. Fluorescence and absorbance measurements were conducted to evaluate the binding interaction between AP3-1 and EGFP. The fluorescence and absorbance trends described by Shui et. al.[64] was also observed in our measurements, validating AP3-1 binding to EGFP. As another control step, we assessed the effectiveness of our designed aggregation protocols to ensure aggregation of EGFP. An increase in light intensity from SLS measurements confirmed our use of TFE (chemical induced aggregation) and glass beads with shaking (mechanical agitation) as successful methods to induce the formation of EGFP aggregates.

To determine the effect of AP3-1 on EGFP aggregation, we continued to use and compare SLS measurements. We observed an increase in static light intensity values in EGFP solutions with AP3-1. This increase can be attributed to two possible scenarios: 1) the presence of large, insoluble aggregated structures or 2) an increased population of soluble structures. To distinguish these potential sources of increased light scattering, we centrifuged the samples and studied the supernatant of these aggregation solutions, which would be considered to contain soluble structures. SLS measurements determined that solutions containing AP3-1 maintained a larger population of soluble structures compared to solutions without AP3-1. The solubility of these structures indicated that they are

possibly intermediate structures (i.e. oligomeric complexes). Interestingly, an analogous product and population of oligomeric structures has been observed in the presence of aptamers in our other study [Tran et.al., in preparation]. The increased presence of oligomeric structures due to addition of an aptamer provides evidence for the utility of aptamers as potential modulators of protein aggregation for future studies.

The results collected in this study complement previous work done on the mechanistic effect of aptamers on protein aggregation [Tran et. al., in preparation]. It is possible that the presence of soluble, oligomeric species in a mixture of AP3-1 and EGFP may be related to the inhibition of EmGFP aggregation that was previously observed (unpublished data, T. Nguyen). However, further work should be done in order to understand that relationship. This work is another addition to the growing research studying whether aptamers can act as modulators to address the concerns of protein aggregation that are significant for biomedical industry.

4.4 Methods and Materials

Protein Expression and Purification of EGFP: EGFP-pBAD (5) vector was used to express Enhanced GFP (EGFP). EGFP-pBAD was a gift from Michael Davidson(Addgene plasmid #54762 ; `http://n2t.net/addgene:54762` ; RRID:Addgene_54762). The EGFP-pBAD plasmid construct was transformed into *Escherichia coli* BL21(DE3) competent cells (New England Biolabs). Expression of protein began with a 37°C incubation of transformed cells. When the $OD_{600} = 0.6$ then, the culture was induced with 1mM isopropyl β-D-1-thiogalactopyranoside (IPTG; Sigma-Aldrich). Cell cultures were harvested at 5,000xg for 15 minutes. Pelleted cells were resuspended in a lysis buffer (50mM NaH_2PO_4, 300mM NaCl and 10mM Imidazole, pH 8.0). Lysed samples were centrifuged at 30,000 xg for 30 minutes to pellet cell debris. Supernatant was filtered using a 0.2μm vacuum filter (Corning) prior to purification. A 5mL HisTrap HP column (GE Healthcare Life Sciences) was used to purify protein. Wash buffer (50mM NaH2PO4, 300mM NaCl and 20mM Imidazole, pH 8.0) and elution buffer (50mM NaH_2PO_4, 300mM NaCl and 175mM Imidazole, pH 8.0) were used to elute protein off column. Fractions containing the expected protein were collected and dialyzed in 1x PBS buffer. Aliquots of protein were divided and stored in -80°C.

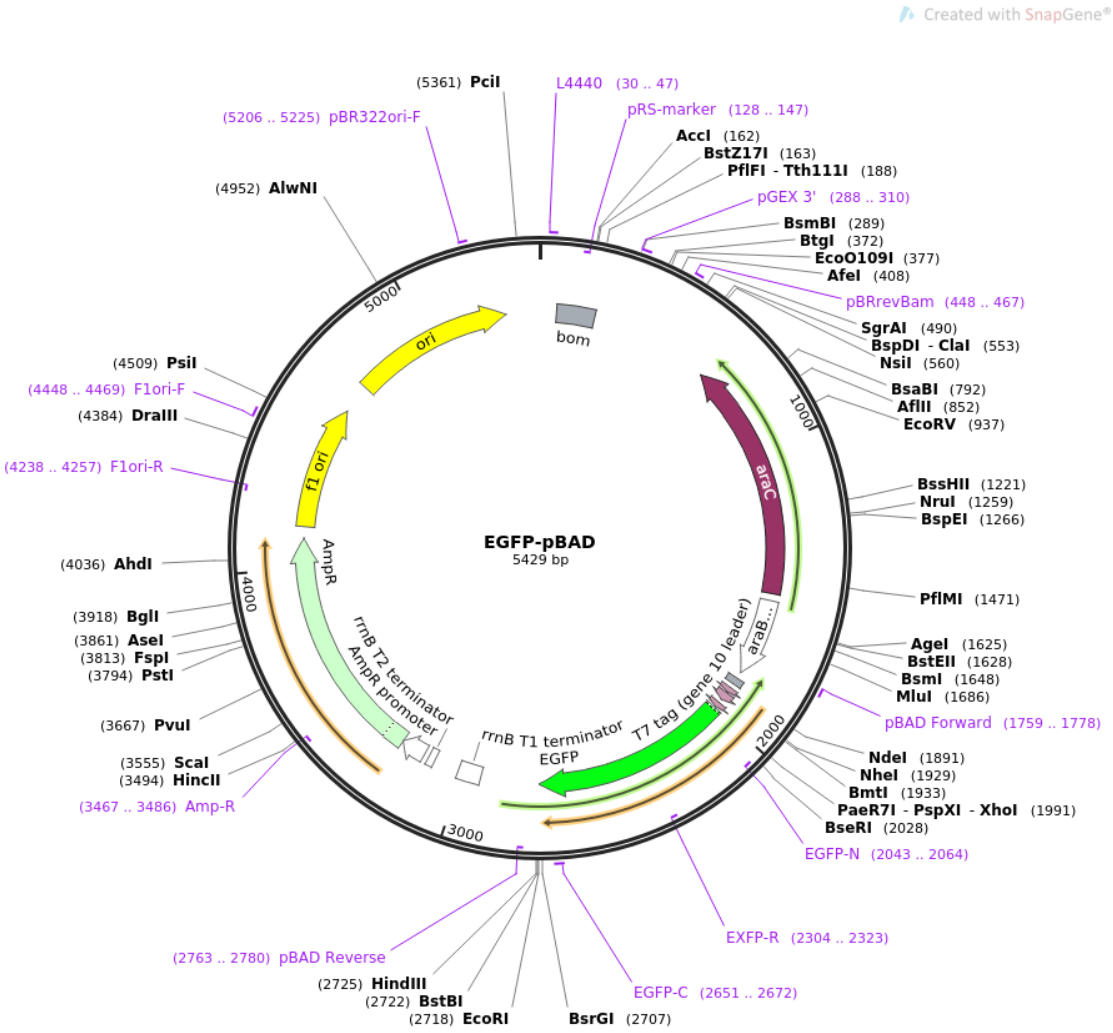

Figure 5: Plasmid map of EGFP contruct[71]

Synthesis of AP3-1 aptamer: The sequence of AP3-1 was collected from Shui et. al.[64]. The DNA template and primers (forward and reverse) were used to generate the RNA sequence of AP3-1 aptamer1.

Name	Sequence (5'—3')
AP3-1 DNA Template	GGGAG CACGA TGGCG TGGCG AATTG GGTGG GGAAA GTCCT TAAAA GAGGG CCACC ACAGA AGCAA TGGGC TTCTG GACTC GGT
AP3-1 Forward Primer	GATAA TACGA CTCAC TATAG GGAGC AC
AP3-1 Reverse Primer	ACCGA GTCCA GAAGC CCA

Table 1: DNA sequences used in this study to generate the RNA aptamer AP3-1.

DNA sequences were purchased from Integrated DNA Technologies (IDT). Phusion High-Fidelity PCR Master Mix with HF Buffer (New England Biolabs) was used to PCR amplify the DNA template for transcription purposes. The PCR product was gel purified (8% native-PAGE). *In vitro* transcription of AP3-1 aptamer was synthetiszed using a HIScribe T7 Quick High Yeild RNA synthesis kit. Following transcription, the "crush and soak" method was used to recover AP3-1 along with an ethanol precipitation for 1 hour at -20°C to precipitate out AP3-1. The solution was centrifuged at 20,000 xg at 4°C for 1 hour. The supernatant was removed and pellets, containing AP3-1, were washed with 70% cold ethanol and dried in air for 2 hours. When testing was ready, RNA pellets were resuspended in RNase-free dionized water.

Binding Assay: Fluorescence and absorbance was used to confirm binding between AP3-1 and EGFP. These two methods were described in Shui et. al. **??**

Fluorescence Assay: A variation of AP3-1 concentration (0-250nM) was incubated with EGFP after vortexing (200nM). Samples were incubated for 30 minutes at 37C before fluorescence measurements. A fluorometer (Horiba Fluoromax 4C) was used to excite samples at 460nm and emission was collected at 490-600nm. The emission values were

compared to determine AP3-1 binding.

Absorbance Assay: An absorbance scan ranging from 350nm to 650nm was performed to determine binding of AP3-1 to EGFP. Samples containing EGFP (200nM) and AP3-1 (5μM) were incubated at 37C for 30 minutes. After incubation, sample absorptions were measured in IMPLEN P300 nanophotometer. The absorption values of the two conditions were compared to determine AP3-1 binding.

Aggregation assay: In this study, there were three methods used to stress EGFP and induce aggregation: chemical induction, mechanical agitation and lyophilization.

Chemically induced protien aggregation: 2,2,2-trifluoroethanol (TFE) was used to induce aggregation of EGFP. TFE was used at 40%(w/v) to chemically aggregate EGFP. Samples with TFE were incubated for 25 minutes. Finally, samples were mixed by vortex and aggregation was determined by SLS. Unless specified otherwise, studies using TFE induced aggregation used 5 μM EGFP and an AP3-1 concentration of 7.2μM.

Mechanical agitation: Agitation was performed in a Tecan M200 Pro instrument. Samples were added into a 96-well plate (Corning) with a 3mm glass bead (Fischer Scientific). A program was designed to continually agitate the samples for a specified time with 10 second break after every 30 minutes. All aggregation assays were performed at 37°C with agitation by orbital shaking of 2 mm (280 rpm).

Lyophilization method: A volume of 1ml of EGFP (with or without AP3-1(1μM)) was flash-freezed using liquid nitrogen for 30 minutes. Samples were transferred to a lyophilizer (Freeze Zone 4.5, Labconco) and an overnight program was set to lyophilize the samples. Samples were resuspended in 125 µL buffer containing 1x PBS (10mM phosphate buffer, 137mM NaCl and 2.7mM KCl, pH 7.4) and 5 mM MgCl2 . These samples were then mechanically agitated using the method described in the 'Mechanical Agitation' method.

Static Light Scattering (SLS): SLS data of the aggregated samples were measured

using the Zetasizer Nano ZSP (Malvern Instruments, UK) at room temperature. 15 μL of the samples were collected in low volume quartz cuvette (Malvern ZEN2112) and instrument provided molecular weight set program was used to extract the static scattering intensity of the respective samples.

Chapter 5

Final Thoughts and Future Works

Protein aggregation is a growing concern and methods to mitigate aggregation have become a priority. In the studies presented here, we established a potential mechanism behind the inhibitory effect of aptamers on two different protein aggregation models, α-synuclein and GFP. In both cases, we observed an increase in population of intermediate structures (i.e., oligomers) when aptamers were present. Further investigation into α-synuclein aggregation determined that the oligomers developed in the presence of TSO508 (α-synuclein aptamer) did not promote aggregation (i.e., were incapable of seeding aggregation), establishing that the oligomers present were off-pathway. These results led us to posit a mechanism in which aptamers modulate α-synuclein aggregation by promoting the development of off-pathway oligomers. While we did not further investigate the GFP case, the presence of oligomeric structures suggests that a similar mechanism might be at work. The development of off-pathway oligomeric species by aptamers might stimulate additional work to investigate the structural properties of these aptamer-oligomer complexes. Additionally, these studies suggest an alternative use of aptamers as modulatory tools, especially regarding protein aggregation. Furthermore, the work reported here emphasizes the modulatory capabilities of aptamers and encourages

continued research to strengthen the therapeutic potential of aptamers.

Chapter 6

Supplementary Materials

6.1 Appendix for Chapter 2

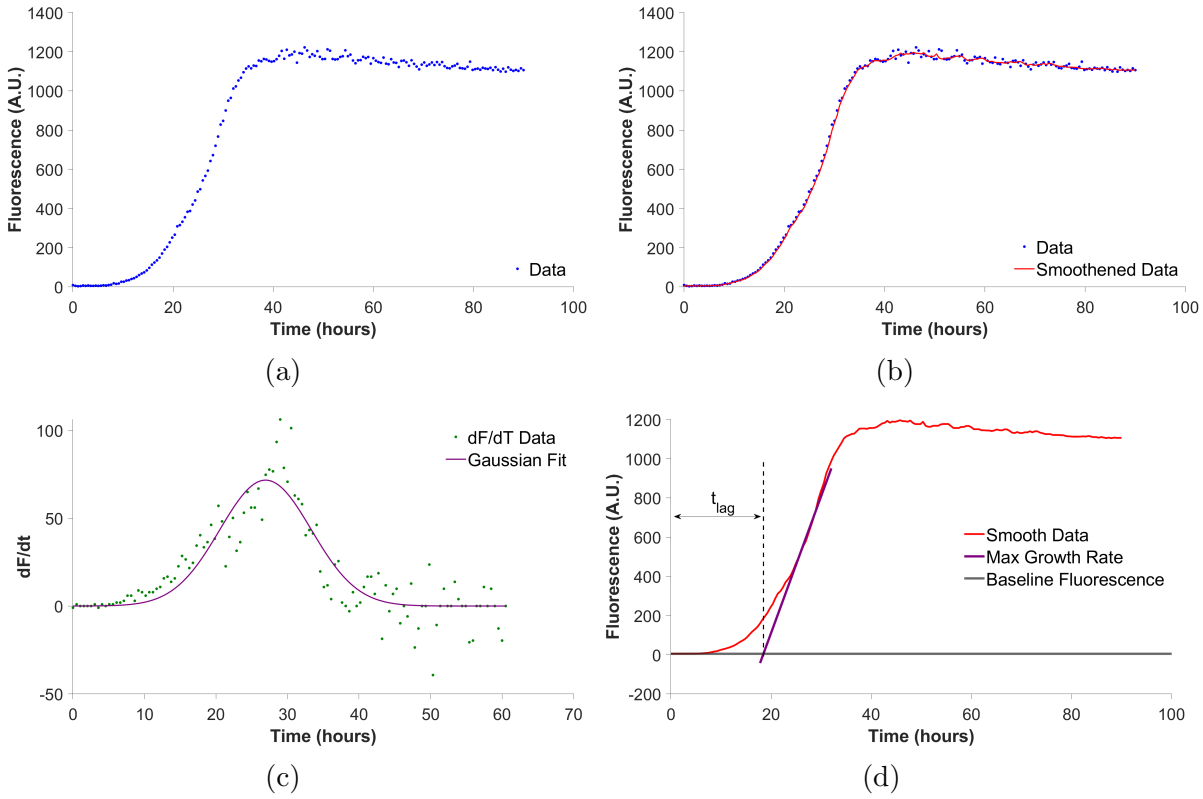

Figure S1: Model-independent (MI) analysis was conducted individually on each data set (n=6) for each condition (9 separate conditions). Fluorescence of Thioflavin T was measured over a period of time (a; blue). Data sets were smoothed using a moving average (b, red). The first derivative was calculated on the smoothed data (c, green) and fit to a Gaussian curve (c, purple), the center of which was taken as the peak time. To determine t_{lag} (d), the intercept between the growth rate tangent at the peak time (purple line) and the average of the starting fluorescence (gray line) was calculated. The x-coordinate of the intercept is the t_{lag} value. Further representation of t_{lag} is shown by the dotted vertical line expressing that t_{lag} is a value of time.

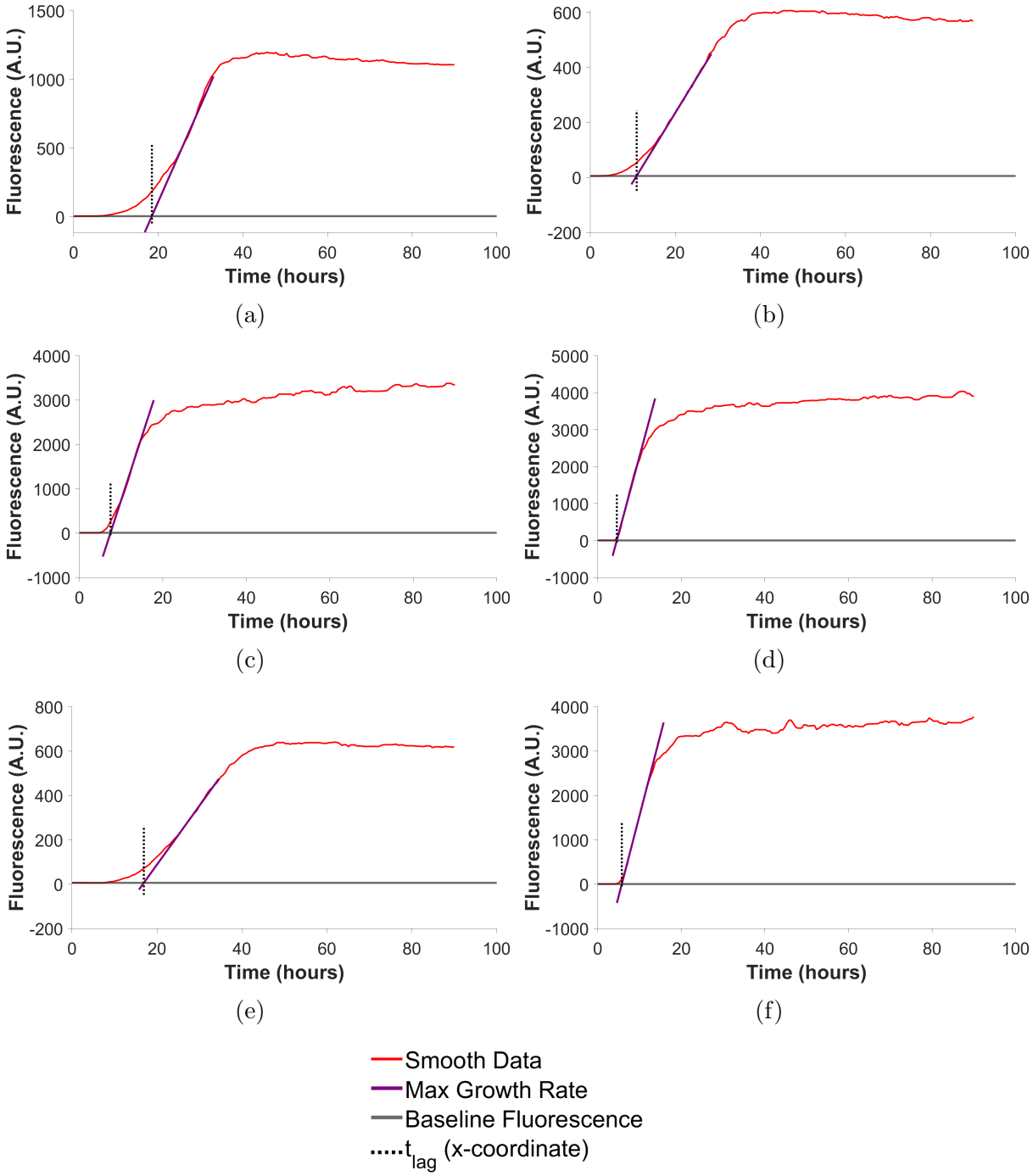

Figure S2: Determination of t_{lag} and growth rate of α-synuclein (140μ) aggregation (a-f). t_{lag} and max growth rate are determined by MI method, further depicted in S1.

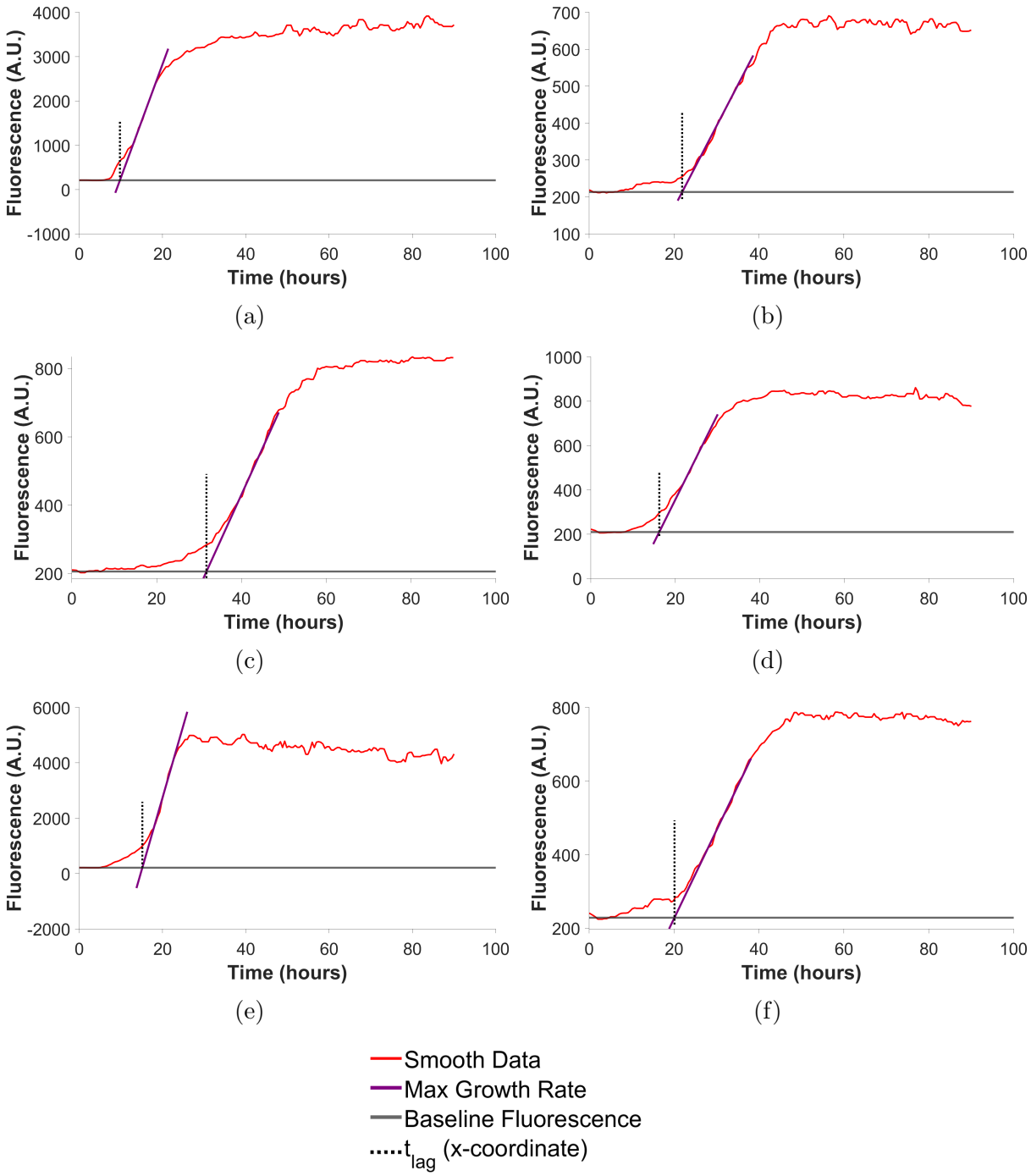

Figure S3: Determination of t_{lag} and growth rate of α-synuclein (140μ) with T-SO508(5μM) (a-f). t_{lag} and max growth rate are determined by MI method, further depicted in S1.

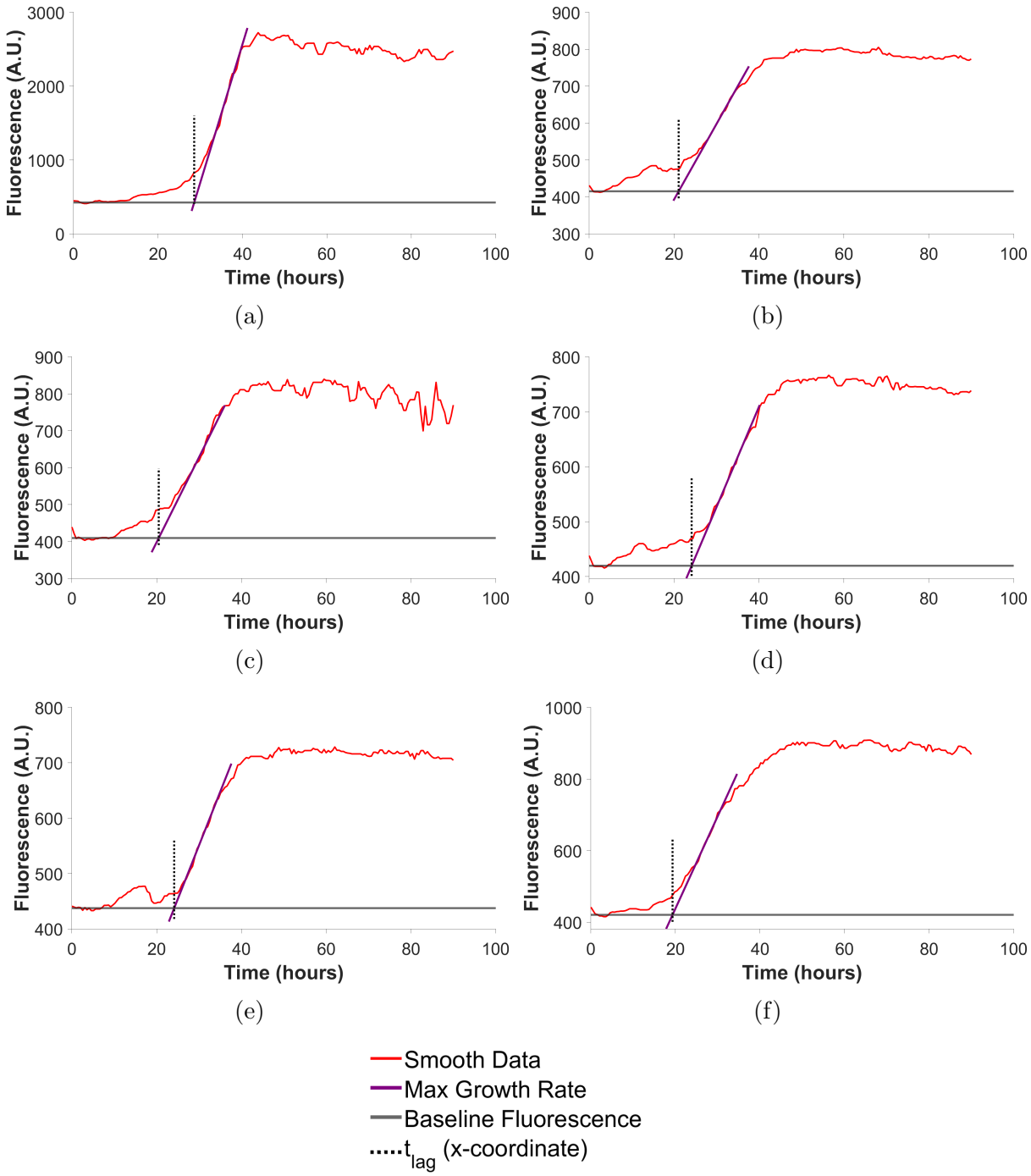

Figure S4: Determination of t_{lag} and growth rate of α-synuclein (140μ) with T-SO508(10μM) (a-f). t_{lag} and max growth rate are determined by MI method, further depicted in S1.

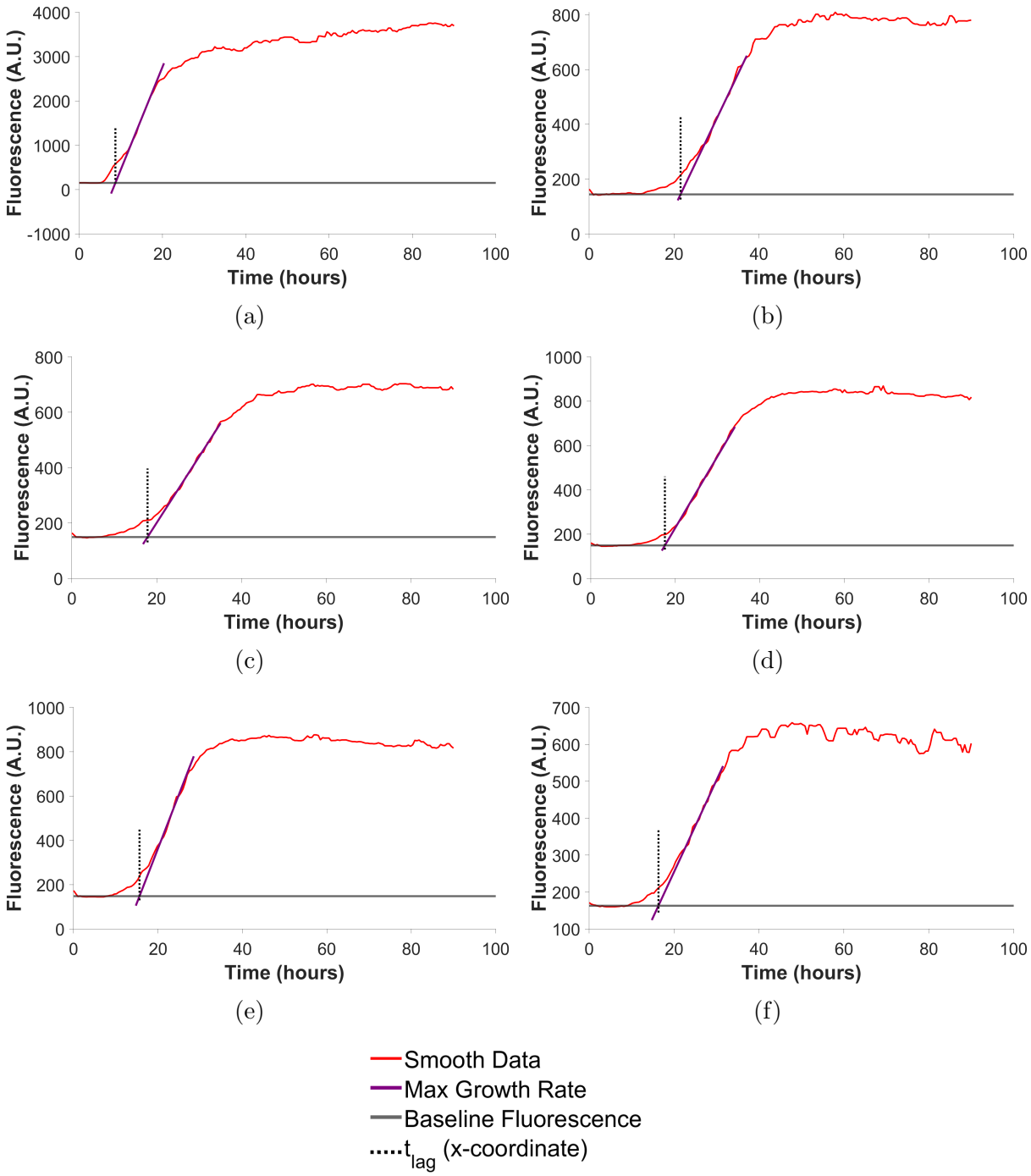

Figure S5: Determination of t_{lag} and growth rate of α-synuclein (140μ) with T-SO530(5μM) (a-f). t_{lag} and max growth rate are determined by MI method, further depicted in S1.

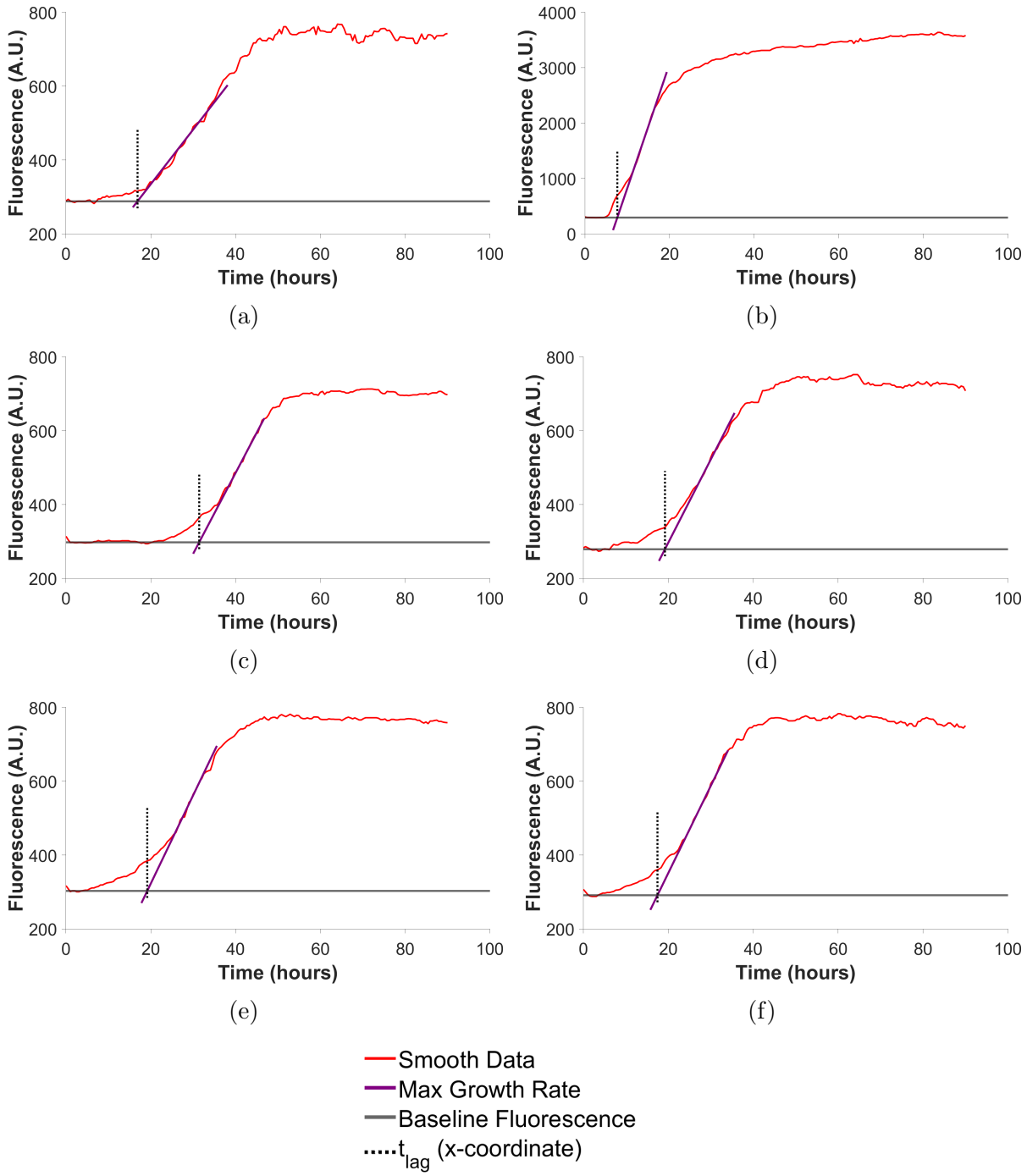

Figure S6: Determination of t_{lag} and growth rate of α-synuclein (140μ) with T-SO530(10μM) (a-f). t_{lag} and max growth rate are determined by MI method, further depicted in S1.

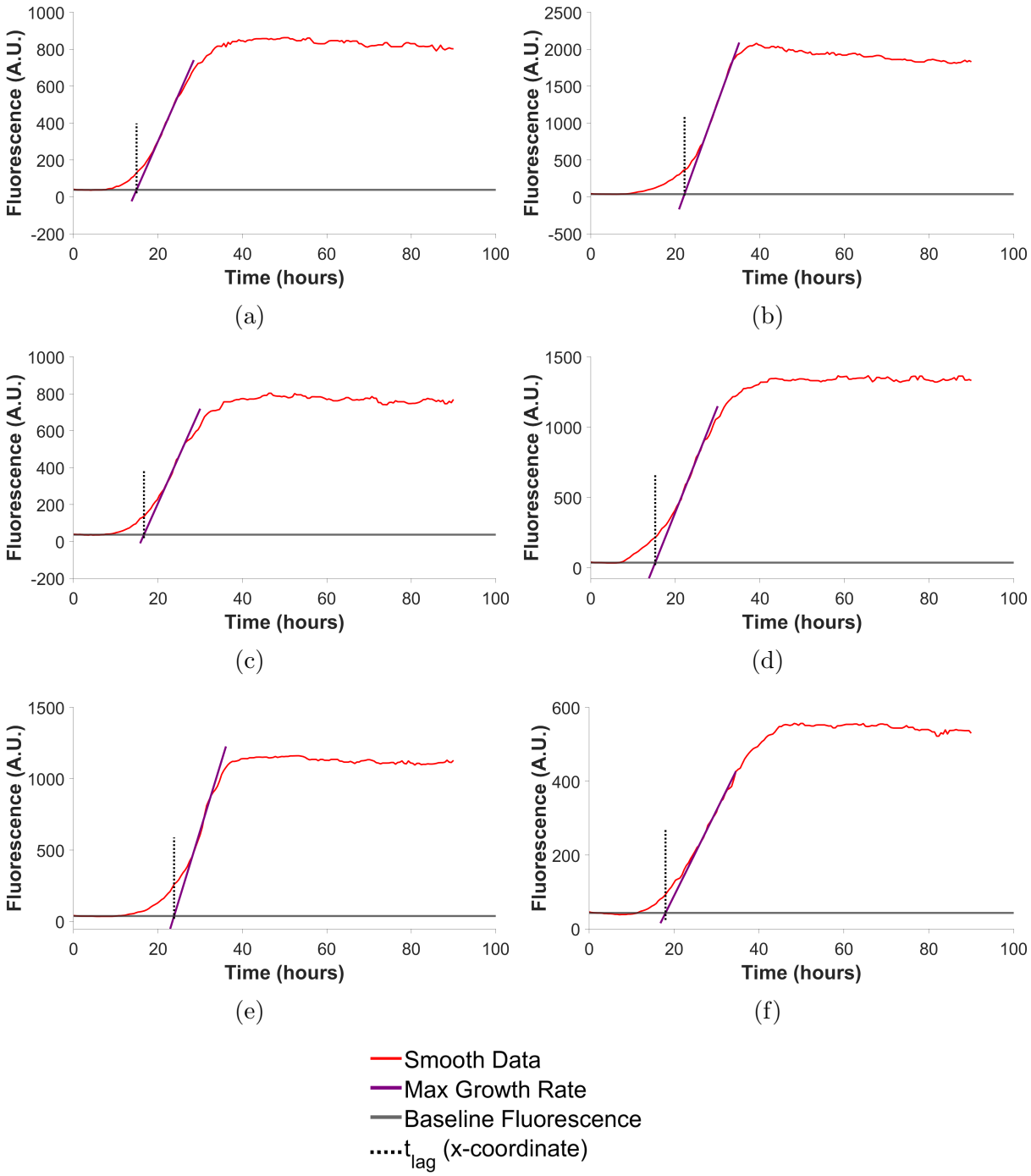

Figure S7: Determination of t_{lag} and growth rate of α-synuclein (140μ) with Thrombin binding aptamer(5μM) (a-f). t_{lag} and max growth rate are determined by MI method, further depicted in S1.

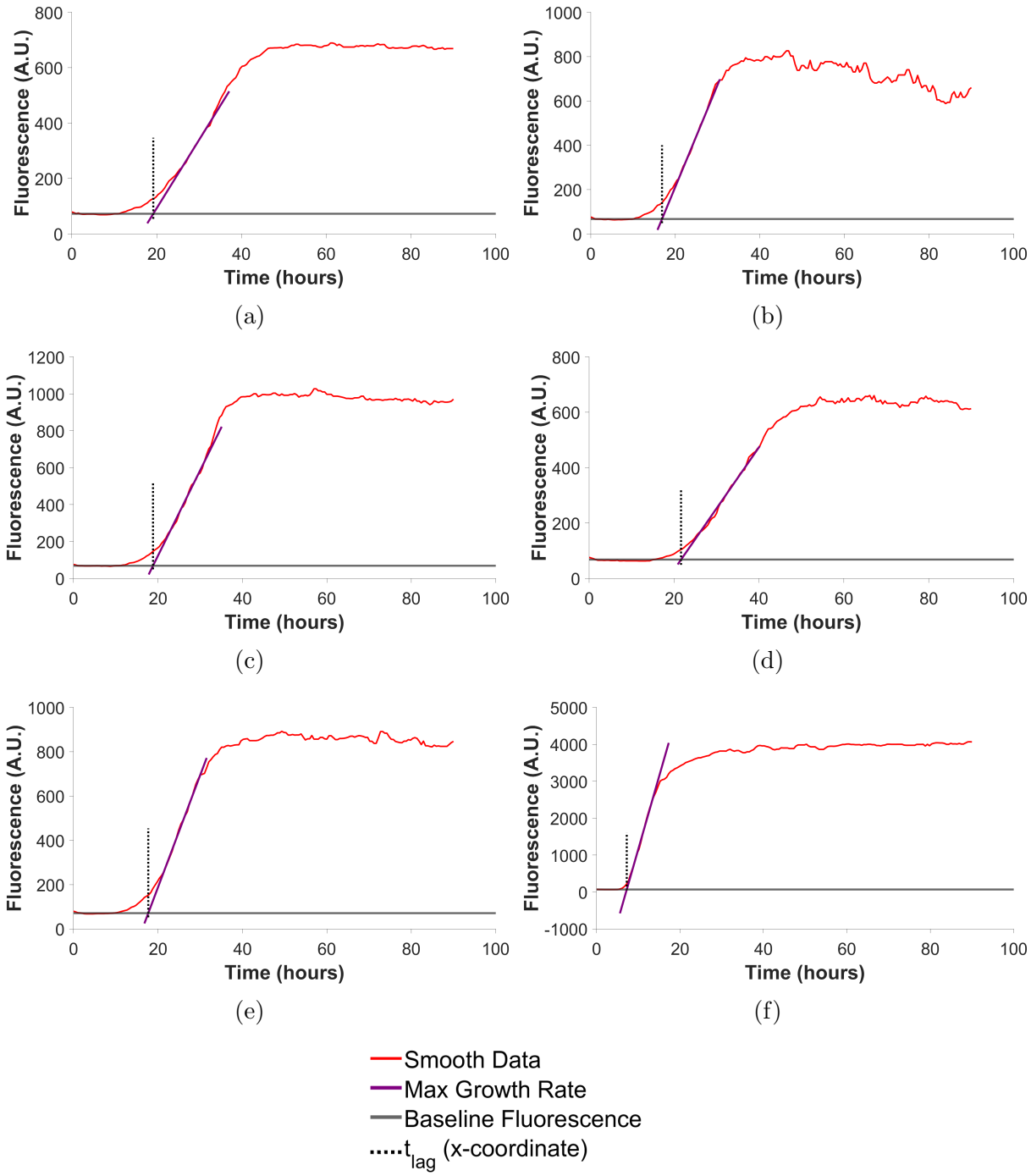

Figure S8: Determination of t_{lag} and growth rate of α-synuclein (140μ) with Thrombin binding aptamer(10μM) (a-f). t_{lag} and max growth rate are determined by MI method, further depicted in S1.

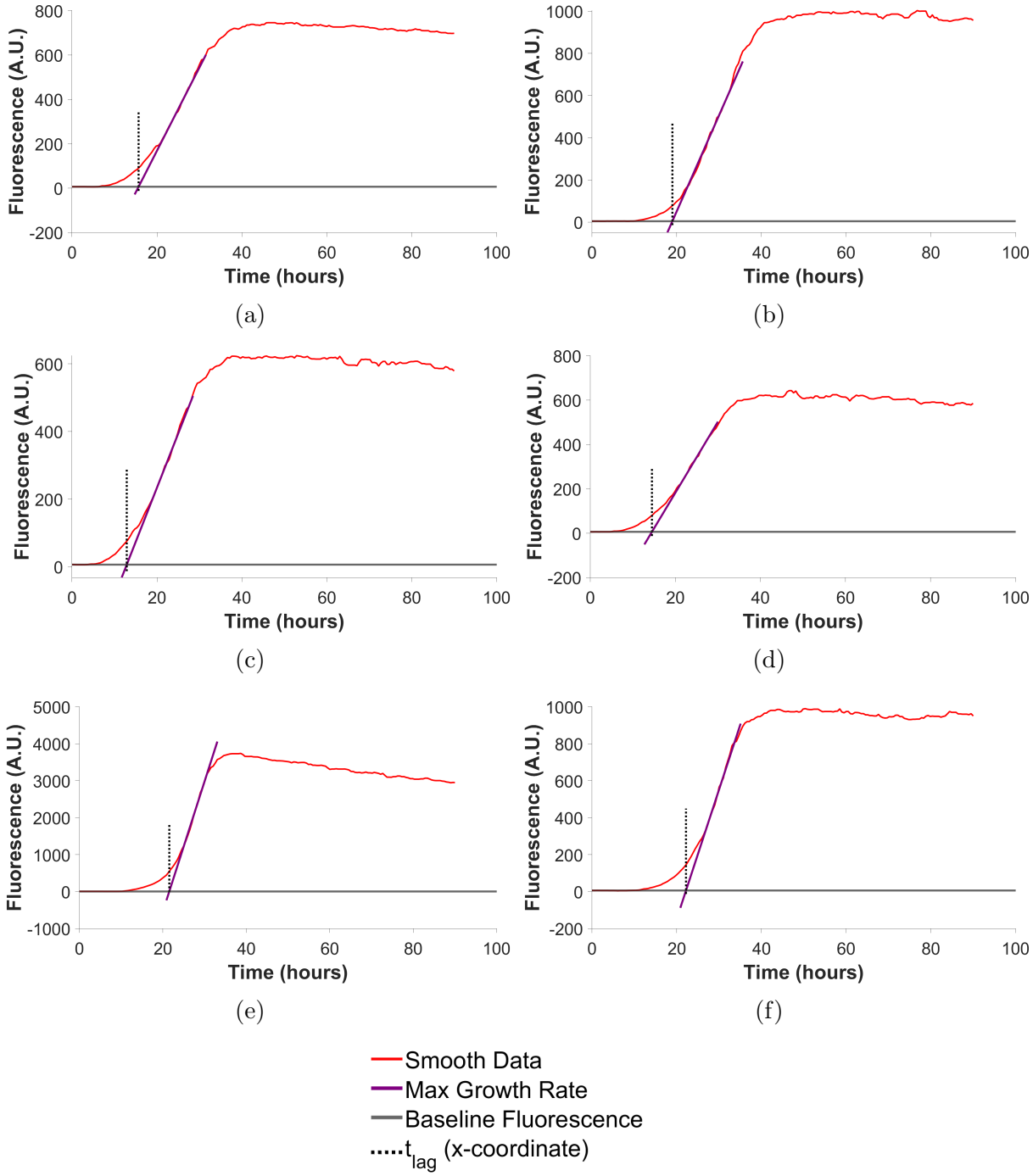

Figure S9: Determination of t_{lag} and growth rate of α-synuclein (140μ) with PolyT (5μM) (a-f). t_{lag} and max growth rate are determined by MI method, further depicted in S1.

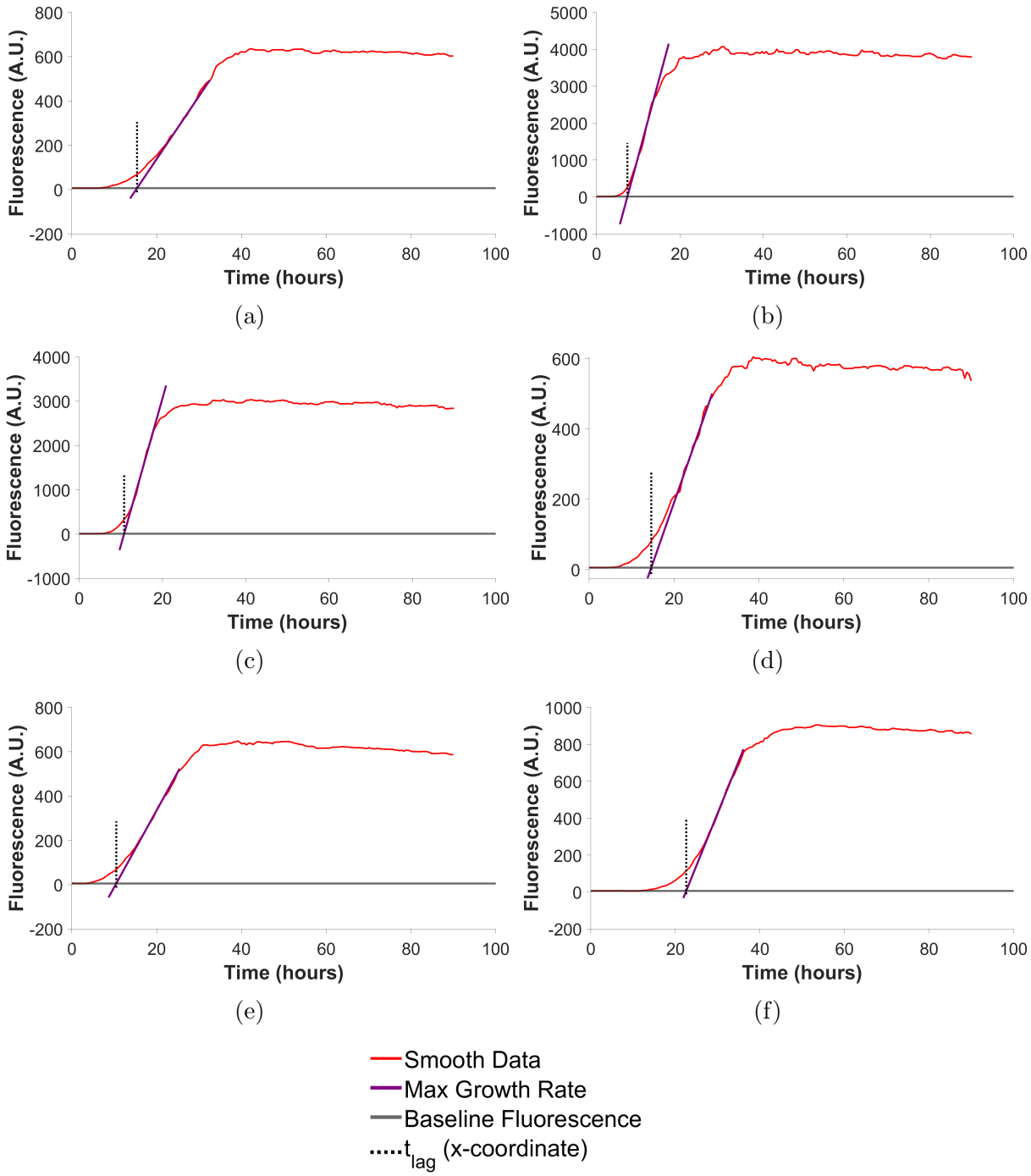

Figure S10: Determination of t_{lag} and growth rate of α-synuclein (140μ) with PolyT (10μM) (a-f). t_{lag} and max growth rate are determined by MI method, further depicted in S1.

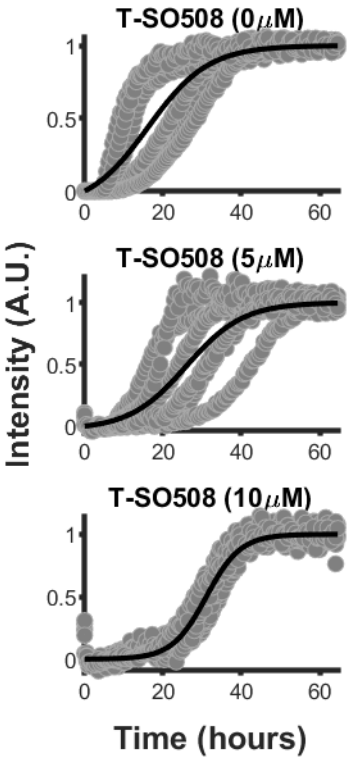

Figure S11: Data fitting to the Finke-Watzky two-step aggregation model, in the presence of T-SO508 aptamer in the concentrations specified (0 μM, 5 μM, and 10 μM). The gray dots represent normalized data taken at each condition (n=6), while the black solid line represents the fitted data from all data collected at the specified condition.

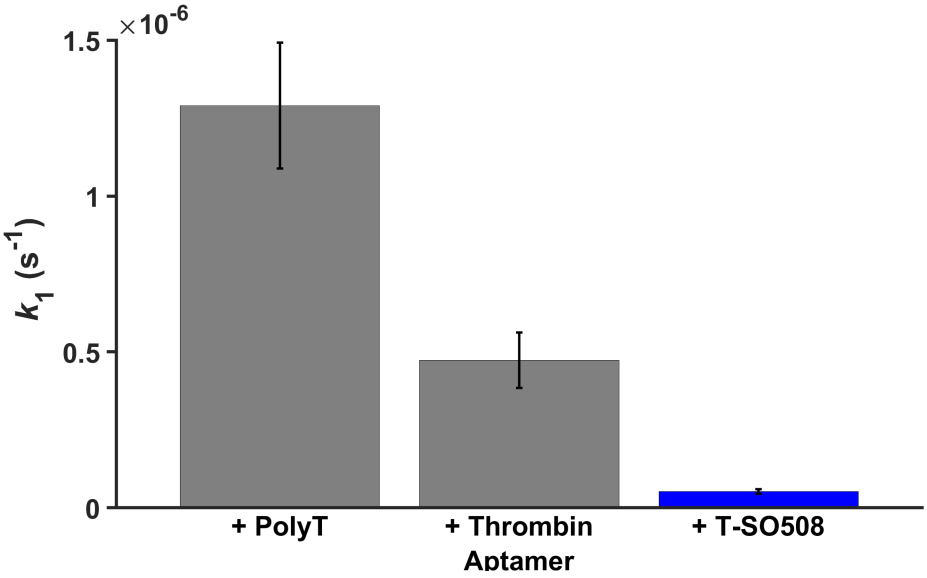

(a)

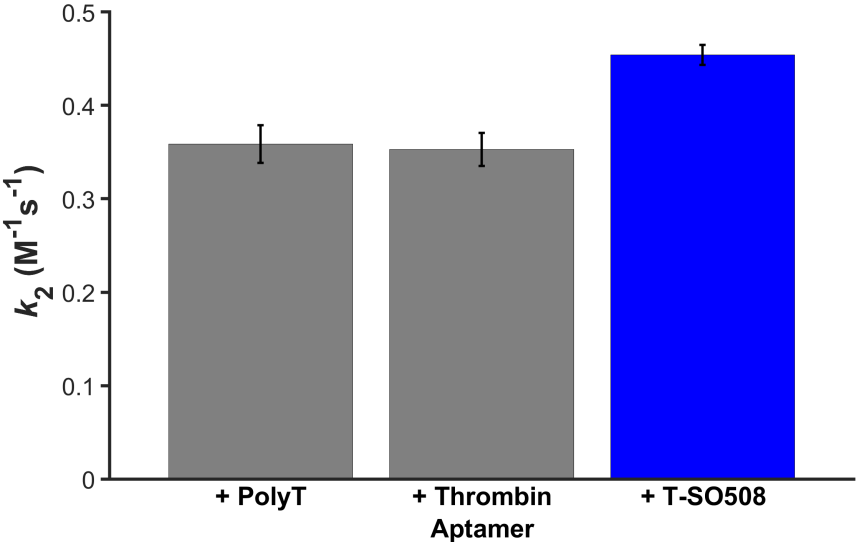

(b)

Figure S12: Finke-Watzky analysis determined the global fits of k_1 and k_2, which supports the observation that T-SO508 prolongs the lag phase as seen by comparing various DNA sequences (thrombin-binding aptamer and 24-mer poly-T). Samples contained 140μM α-synuclein, 60 μM ThT, and 10 μM of T-SO508, thrombin aptamer, or poly-T. Error bars represent the fitted parameter standard error for each condition.

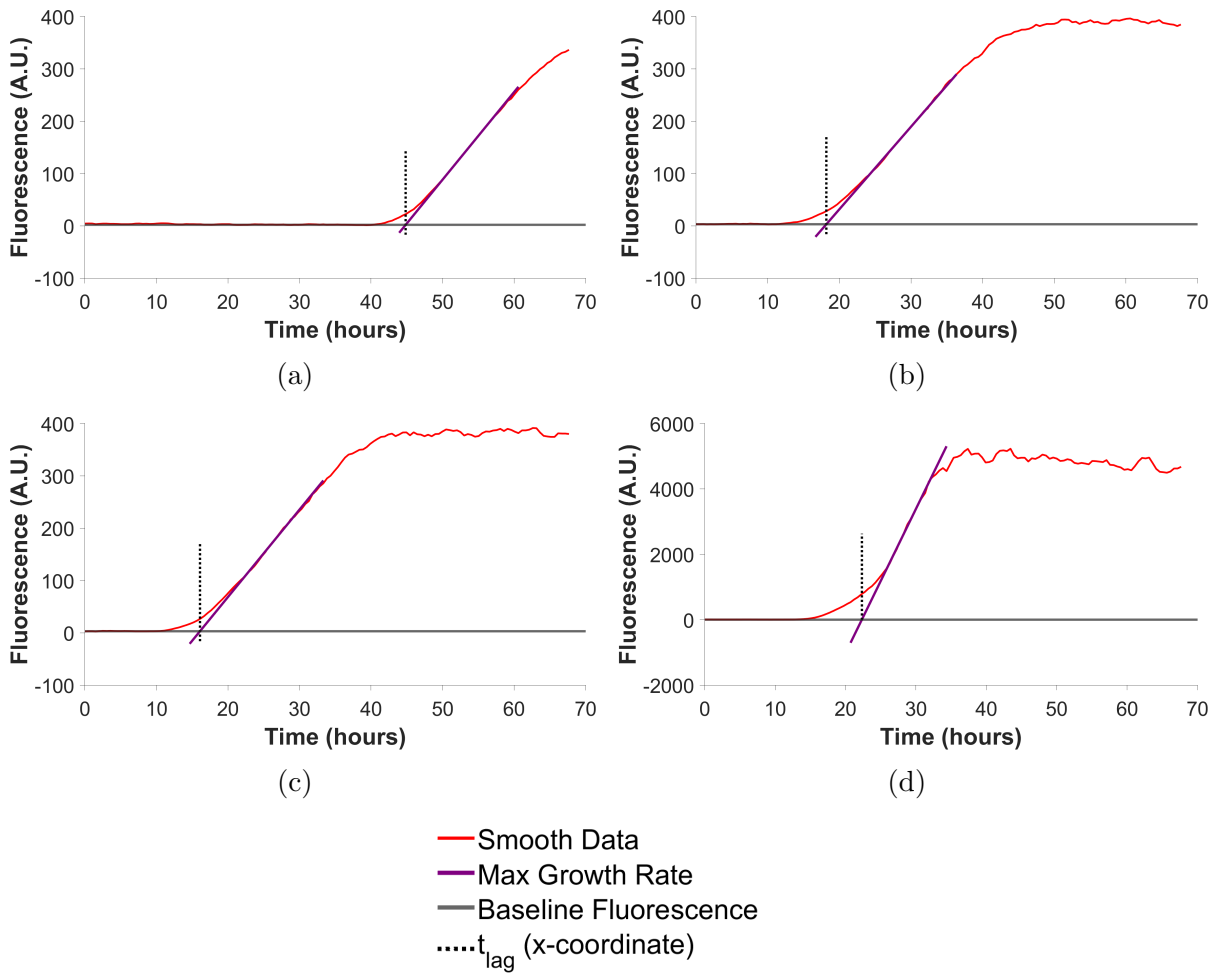

Figure S13: Determination of t_{lag} and growth rate of α-synuclein (70μM) (a-d). t_{lag} and max growth rate are determined by MI method, further depicted in S1.

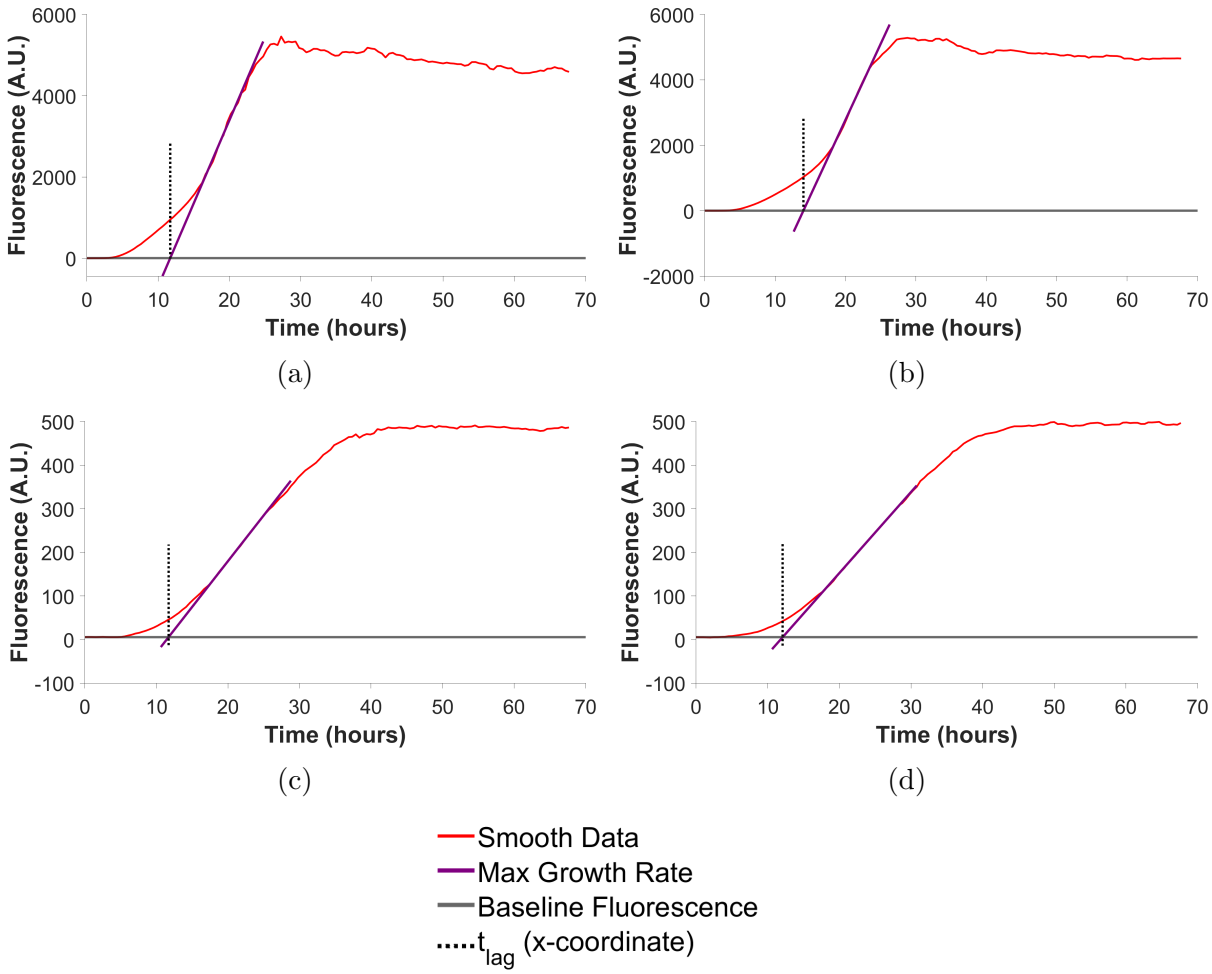

Figure S14: Determination of t_{lag} and growth rate of α-synuclein (70μM) inoculated with α-synuclein seeds. Preparation of seeds described in methods section of Chapter 2. (a-d). t_{lag} and max growth rate are determined by MI method, further depicted in S1.

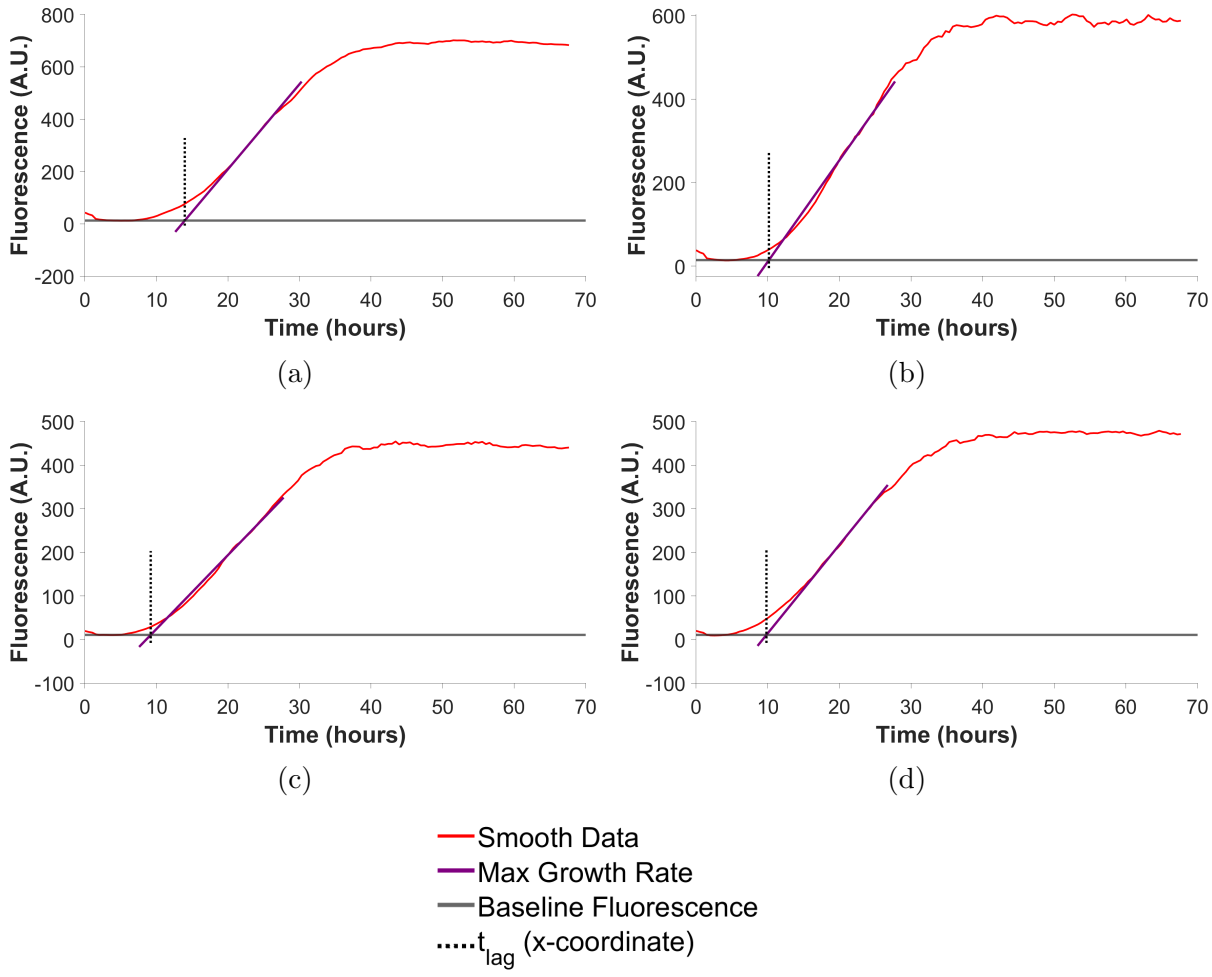

Figure S15: Determination of t_{lag} and growth rate of α-synuclein (70μM) inoculated with seeds formed in the presence of Thrombin binding aptamer (70μM). Preparation of seeds described in methods section of Chapter 2. (a-d). t_{lag} and max growth rate are determined by MI method, further depicted in S1.

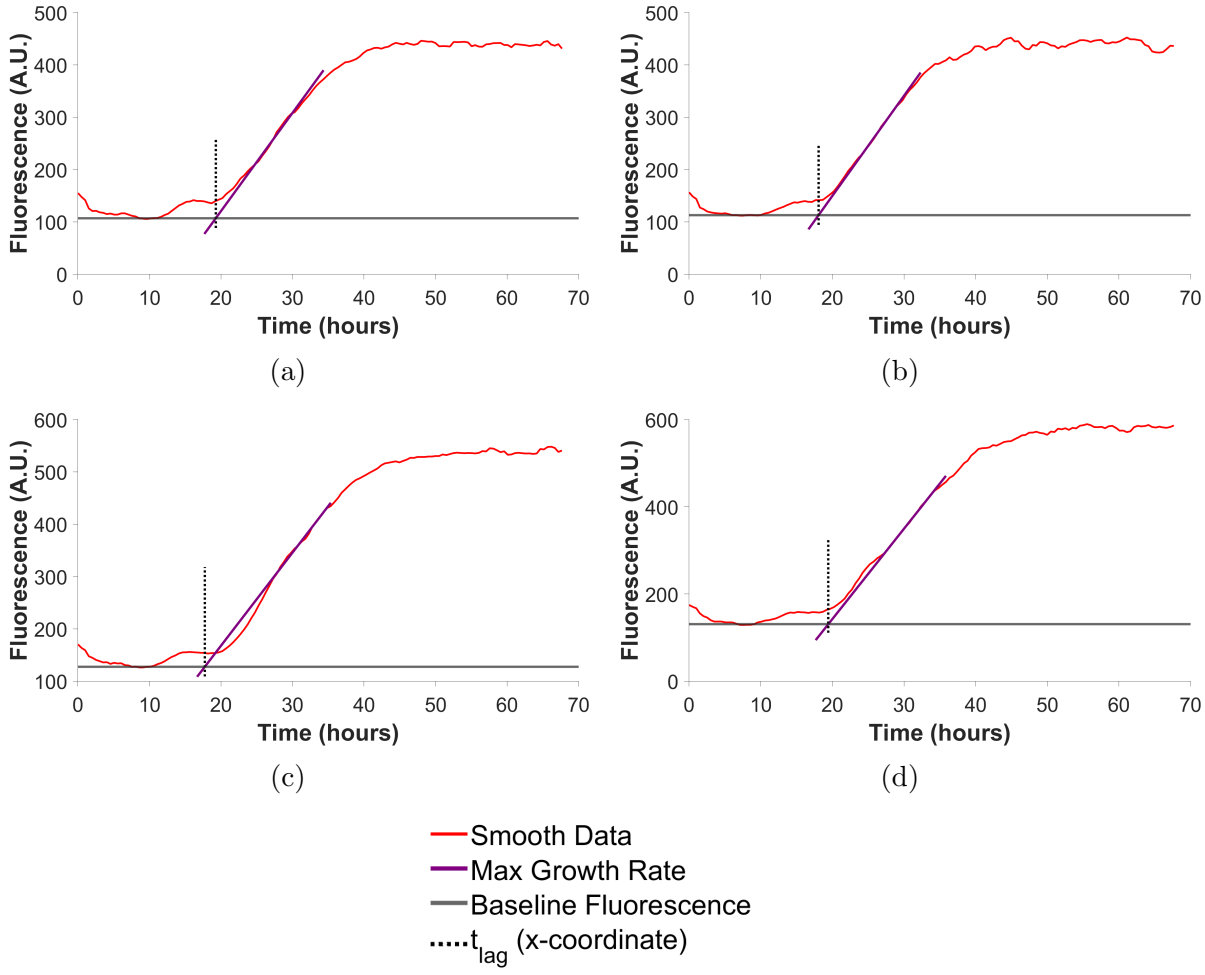

Figure S16: Determination of t_{lag} and growth rate of α-synuclein (70μM) inoculated with seeds formed in the presence of T-SO508(45μM). Preparation of seeds described in methods section of Chapter 2. (a-d). t_{lag} and max growth rate are determined by MI method, further depicted in S1.

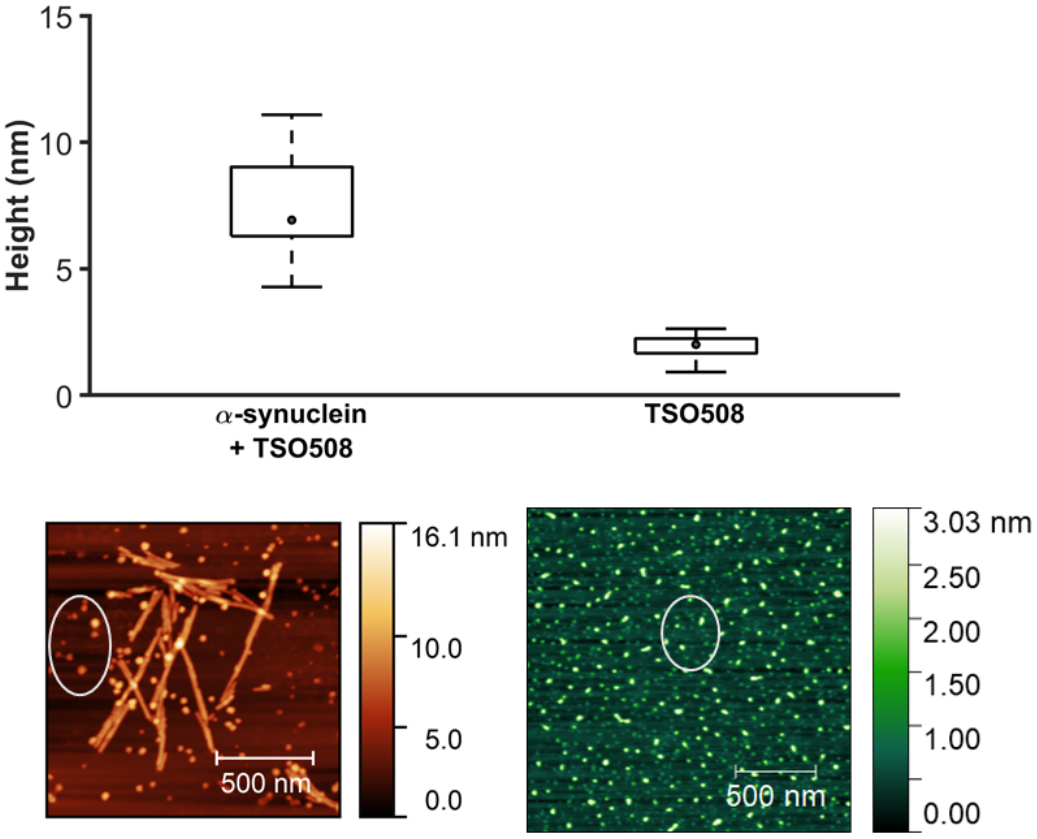

Figure S17: Comparison of height profiles of the roughly spherical shapes (examples are outlined by the white circle) found in samples with α-synuclein and TSO508 (left) compared to TSO508 alone (right), determined from AFM images (4c,4b). Error bars represent one standard error (n¿50). The comparison indicates that the structures formed by α-synuclein and TSO508 together are distinct from TSO508 alone.

6.2 Appendix for Chapter 3

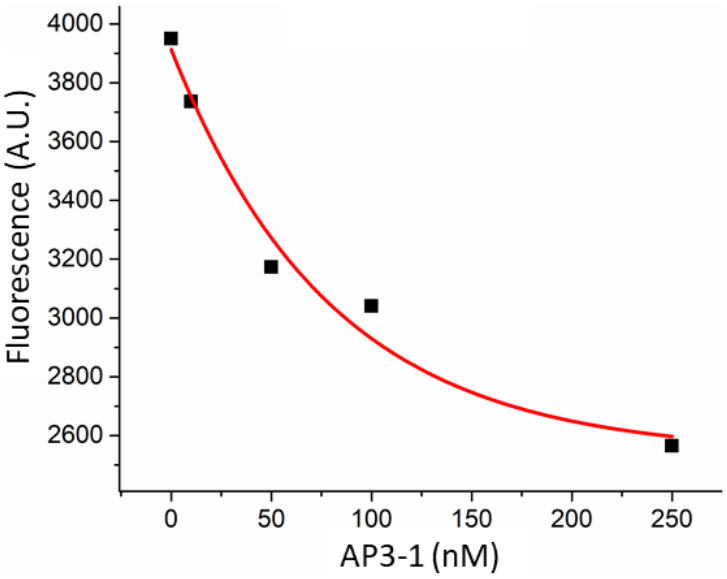

Figure S18: Fluorescence values collected at 505nm showed a decrease in EGFP fluorescence, while AP3-1 concentration was increased. This data supports AP3-1 binding to EGFP.

Bibliography

[1] Marc Zimmer. Green fluorescent protein (GFP): Applications, structure, and related photophysical behavior. *Chemical Reviews*, 102(3):759–781, 2002.

[2] S. James Remington. Green fluorescent protein: A perspective, 2011.

[3] Meenu Wadhwa, Ivana Knezevic, Hye Na Kang, and Robin Thorpe. Immunogenicity assessment of biotherapeutic products: An overview of assays and their utility, 2015.

[4] Frédéric Ducancel and Bruno H. Muller. Molecular engineering of antibodies for therapeutic and diagnostic purposes, 2012.

[5] Parvez Alam, Luc Bousset, Ronald Melki, and Daniel E. Otzen. α-synuclein oligomers and fibrils: a spectrum of species, a spectrum of toxicities. *Journal of Neurochemistry*, 150(5):522–534, 2019.

[6] Leonidas Stefanis. α-Synuclein in Parkinson's disease. *Cold Spring Harbor Perspectives in Medicine*, 2(2):1–23, 2012.

[7] Jacqueline Burré, Manu Sharma, and Thomas C. Südhof. Cell biology and pathophysiology of α-synuclein. *Cold Spring Harbor Perspectives in Medicine*, 8(3), 2018.

[8] Paul J. Carter. Introduction to current and future protein therapeutics: A protein engineering perspective, 2011.

[9] Eva Y. Chi, Sampathkumar Krishnan, Theodore W. Randolph, and John F. Carpenter. Physical stability of proteins in aqueous solution: Mechanism and driving forces in nonnative protein aggregation, 2003.

[10] Hanns Christian Mahler, Wolfgang Friess, Ulla Grauschopf, and Sylvia Kiese. Protein aggregation: Pathways, induction factors and analysis, 2009.

[11] Wei Wang. Protein aggregation and its inhibition in biopharmaceutics. *International Journal of Pharmaceutics*, 289(1-2):1–30, 2005.

[12] Hiroyuki Hamada, Tsutomu Arakawa, and Kentaro Shiraki. Effect of Additives on Protein Aggregation. *Current Pharmaceutical Biotechnology*, 10(4):400–407, 2009.

[13] Massimo Stefani and Christopher M. Dobson. Protein aggregation and aggregate toxicity: New insights into protein folding, misfolding diseases and biological evolution. *Journal of Molecular Medicine*, 81(11):678–699, 2003.

[14] Parvez Alam, Khursheed Siddiqi, Sumit Kumar Chturvedi, and Rizwan Hasan Khan. Protein aggregation: From background to inhibition strategies, 2017.

[15] Fabrizio Chiti and Christopher M Dobson. Protein Misfolding, Functional Amyloid, and Human Disease. *Annu. Rev. Biochem*, 75:333–66, 2006.

[16] David Eisenberg and Mathias Jucker. The amyloid state of proteins in human diseases, 2012.

[17] Debanjan Kundu, Kumari Prerna, Rahul Chaurasia, Manoj Kumar Bharty, and Vikash Kumar Dubey. Advances in protein misfolding, amyloidosis and its correlation with human diseases. *3 Biotech*, 10(5):193, 2020.

[18] Catriona A. McLean, Robert A. Cherny, Fiona W. Fraser, Stephanie J. Fuller, Margaret J. Smith, Konrad Beyreuther, Ashley I. Bush, and Colin L. Masters. Soluble pool of Aβ amyloid as a determinant of severity of neurodegeneration in Alzheimer's disease. *Annals of Neurology*, 46(6):860–866, 1999.

[19] Lih Fen Lue, Yu Min Kuo, Alex E. Roher, Libuse Brachova, Yong Shen, Lucia Sue, Thomas Beach, Janice H. Kurth, Russel E. Rydel, and Joseph Rogers. Soluble amyloid β peptide concentration as a predictor of synaptic change in Alzheimer's disease. *American Journal of Pathology*, 155(3):853–862, 1999.

[20] Wim Jiskoot, Theodore W. Randolph, David B. Volkin, C. Russell Middaugh, Christian Schöneich, Gerhard Winter, Wolfgang Friess, Daan J.A. Crommelin, and John F. Carpenter. Protein instability and immunogenicity: Roadblocks to clinical application of injectable protein delivery systems for sustained release, 2012.

[21] F. Ulrich Hartl and Manajit Hayer-Hartl. Protein folding. Molecular chaperones in the cytosol: From nascent chain to folded protein, 2002.

[22] Michael S Lawrence, Kevin J Phillips, and David R Liu. Supercharging proteins can impart unusual resilience. *Journal of the American Chemical Society*, 129(33):10110–10112, 2007.

[23] Shantanu V Lale, Monu Goyal, and Arvind K Bansal. Development of lyophilization cycle and effect of excipients on the stability of catalase during lyophilization. *International journal of pharmaceutical investigation*, 1(4):214–21, 2011.

[24] Serge N Timasheff. The Stabilization of Proteins by Sucrose*. 256(14):7193–7201, 1981.

[25] Motonori Kudou, Kentaro Shiraki, Shinsuke Fujiwara, Tadayuki Imanaka, and Masahiro Takagi. Prevention of thermal inactivation and aggregation of lysozyme by polyamines. *European Journal of Biochemistry*, 270(22):4547–4554, 2003.

[26] Shermeen A Abbas, Vikas K Sharma, Thomas W Patapoff, and Devendra S Kalonia. Opposite effects of polyols on antibody aggregation: Thermal versus mechanical stresses. *Pharmaceutical Research*, 29(3):683–694, 2012.

[27] Andrew D Ellington and Jack W Szostak. In vitro selection of RNA molecules that bind specific ligands. *Nature*, 346(6287):818–822, 1990.

[28] Debra L Robertson and Gerald F Joyce. Selection in vitro of an RNA enzyme that specifically cleaves single-stranded DNA. *Nature*, 344(6265):467–468, 1990.

[29] Craig Tuerk and Larry Gold. Systematic evolution of ligands by exponential enrichment: RNA ligands to bacteriophage T4 DNA polymerase. *Science*, 249(4968):505–510, 1990.

[30] Juan Zhang, Lihua Wang, Dun Pan, Shiping Song, Freddy Y.C. Boey, Hua Zhang, and Chunhai Fan. Visual cocaine detection with gold nanoparticles and rationally engineered aptamer structures. *Small*, 4(8):1196–1200, 2008.

[31] Zhengbo Chen, Yuan Tan, Chenmeng Zhang, Lu Yin, He Ma, Nengsheng Ye, Hong Qiang, and Yuqing Lin. A colorimetric aptamer biosensor based on cationic polymer and gold nanoparticles for the ultrasensitive detection of thrombin. *Biosensors and Bioelectronics*, 56:46–50, 2014.

[32] Xiao Lei Tang, Shi Min Wu, Yan Xie, Neng Song, Qing Guan, Chunhui Yuan, Xiang Zhou, and Xiao Lian Zhang. Generation and application of ssDNA aptamers against glycolipid antigen ManLAM of Mycobacterium tuberculosis for TB diagnosis. *Journal of Infection*, 72(5):573–586, 2016.

[33] Stuart L. Fine, Daniel F. Martin, and Peter Kirkpatrick. Pegaptanib sodium, 2005.

[34] Hardik C Jetani, Ankan Kumar Bhadra, Nishant Kumar Jain, and Ipsita Roy. Nucleic Acid Aptamers Stabilize Proteins Against Different Types of Stress Conditions. *J Pharm Sci*, 103:100–106, 2014.

[35] Ravinder Malik and Ipsita Roy. Stabilization of bovine insulin against agitation-induced aggregation using RNA aptamers. *International Journal of Pharmaceutics*, 452(1-2):257–265, 2013.

[36] Daniela Proske, Sabine Gilch, Franziska Wopfner, Hermann M. Schätzl, Ernst-L. Winnacker, and Michael Famulok. Prion-protein-specific aptamer reduces PrPSc formation. *ChemBioChem*, 3(8):717–725, 2002.

[37] Kinjal A Patel, Ratnika Sethi, Anita R Dhara, and Ipsita Roy. Challenges with osmolytes as inhibitors of protein aggregation: Can nucleic acid aptamers provide an answer? *International Journal of Biological Macromolecules*, 100:75–88, 2017.

[38] Tsuyoshi Takahashi, Kosuke Tada, and Hisakazu Mihara. RNA aptamers selected against amyloid beta-peptide (Abeta) inhibit the aggregation of Abeta. *Molecular bioSystems*, 5(9):986–991, 2009.

[39] Ji Hyeon Kim, Eunkyoung Kim, Won Hoon Choi, Jeeyoung Lee, Jung Hoon Lee, Hyojin Lee, Dong Eun Kim, Young Ho Suh, and Min Jae Lee. Inhibitory RNA Aptamers of Tau Oligomerization and Their Neuroprotective Roles against Proteotoxic Stress. *Molecular Pharmaceutics*, 13(6):2039–2048, 2016.

[40] Rajeev K Chaudhary, Kinjal A Patel, Milan K Patel, Radha H Joshi, and Ipsita Roy. Inhibition of aggregation of mutant huntingtin by nucleic acid aptamers in vitro and in a yeast model of Huntington's disease. *Molecular therapy : the journal of the American Society of Gene Therapy*, 23(12):1912–1926, 2015.

[41] Yuan Zheng, Jing Qu, Fenqin Xue, Yan Zheng, Bo Yang, Yongchang Chang, Hui Yang, and Jianliang Zhang. Novel DNA Aptamers for Parkinson's Disease Treatment Inhibit α-Synuclein Aggregation and Facilitate its Degradation. *Molecular Therapy - Nucleic Acids*, 11(June):228–242, 2018.

[42] Xiaoxi Ren, Yun Zhao, Fenqin Xue, Yan Zheng, Haixia Huang, Wei Wang, Yongchang Chang, Hui Yang, and Jianliang Zhang. Exosomal DNA Aptamer Targeting α-Synuclein Aggregates Reduced Neuropathological Deficits in a Mouse Parkinson's Disease Model. *Molecular Therapy - Nucleic Acids*, 17:726–740, 2019.

[43] K Tsukakoshi, K Abe, K Sode, and K Ikebukuro. Selection of DNA aptamers that recognize alpha-synuclein oligomers using a competitive screening method. *Anal Chem*, 84:5542–5547, 2012.

[44] Minna Groenning. Binding mode of Thioflavin T and other molecular probes in the context of amyloid fibrils-current status. *Journal of Chemical Biology*, 3(1):1–18, 2010.

[45] Farjana Yeasmin Khusbu, Xi Zhou, Hanchun Chen, Changbei Ma, and Kemin Wang. Thioflavin T as a fluorescence probe for biosensing applications. *TrAC - Trends in Analytical Chemistry*, 109:1–18, 2018.

[46] M. Ilanchelian and R. Ramaraj. Emission of thioflavin T and its control in the presence of DNA. *Journal of Photochemistry and Photobiology A: Chemistry*, 162(1):129–137, 2004.

[47] See K Suzanne Shoffner, Santiago Schnell, and Suzanne K Shoffner. Showcasing research from the laboratory of Title: Estimation of the lag time in a subsequent monomer addition model for fibril elongation As featured in: Estimation of the lag time in a subsequent monomer addition model for fibril elongation †. *Phys. Chem. Chem. Phys*, 18:21259, 2016.

[48] Aimee M Morris and Richard G Finke. α-Synuclein aggregation variable temperature and variable pH kinetic data: A re-analysis using the Finke–Watzky 2-step model of nucleation and autocatalytic growth. *Biophysical Chemistry*, 140:9–15, 2008.

[49] Murielle A Watzky and Richard G Finke. Transition metal nanocluster formation kinetic and mechanistic studies. A new mechanism when hydrogen is the reductant: Slow, continuous nucleation and fast autocatalytic surface growth. *Journal of the American Chemical Society*, 119(43):10382–10400, 1997.

[50] José Antonio Vázquez. Modeling of chemical inhibition from amyloid protein aggregation kinetics. *BMC Pharmacology and Toxicology*, 15(1), 2014.

[51] R F Macaya, P Schultze, F W Smith, J A Roe, and J Feigon. Thrombin-binding DNA aptamer forms a unimolecular quadruplex structure in solution. *Proceedings of the National Academy of Sciences*, 90(8):3745–3749, 1993.

[52] Helen G Hansma, Irene Revenko, Kerry Kim, and Daniel E Laney. Atomic force microscopy of long and short double-stranded, single-stranded and triple-stranded nucleic acids. Technical Report 4, 1996.

[53] Chiharu Mizuguchi, Miho Nakagawa, Norihiro Namba, Misae Sakai, Naoko Kurimitsu, Ayane Suzuki, Kaho Fujita, Sayaka Horiuchi, Teruhiko Baba, Takashi Ohgita, Kazuchika Nishitsuji, and Hiroyuki Saito. Mechanisms of aggregation and fibril formation of the amyloidogenic N-terminal fragment of apolipoprotein A-I. *Journal of Biological Chemistry*, 294(36):13515–13524, 2019.

[54] Jonathan A. Fauerbach and Thomas M. Jovin. Pre-aggregation kinetics and intermediates of α-synuclein monitored by the ESIPT probe 7MFE. *European Biophysics Journal*, 47(4):345–362, 2018.

[55] Theodore J. Litberg, Brianne Docter, Michael P. Hughes, Jennifer Bourne, and Scott Horowitz. DNA Facilitates Oligomerization and Prevents Aggregation via DNA Networks. *Biophysical Journal*, 118(1):162–171, 2019.

[56] `http://n2t.net/addgene:36046`.

[57] Katerina E. Paleologou, Adrian W. Schmid, Carla C. Rospigliosi, Hai Young Kim, Gonzalo R. Lamberto, Ross A. Fredenburg, Peter T. Lansbury, Claudio O. Fernandez, David Eliezer, Markus Zweckstetter, and Hilal A. Lashuel. Phosphorylation at Ser-129 but not the phosphomimics S129E/D inhibits the fibrillation of α-synuclein. *Journal of Biological Chemistry*, 283(24):16895–16905, 2008.

[58] Origin(Pro), Version 8.5.1. OriginLab Corporation, Northampton, MA, USA.

[59] D Davenport and J. A. C. Nicol. Luminescence in Hydromedusae. *Proceedings of the Royal Society of London. Series B - Biological Sciences*, 144(916):399–411, 1955.

[60] Martin Chalfie, Yuan Tu, Ghia Euskirchen, William W. Ward, and Douglas C. Prasher. Green fluorescent protein as a marker for gene expression. *Science*, 263(5148):802–805, 1994.

[61] Andreas Crameri, Erik A Whitehorn, Emily Tate, and Willem P.C. Stemmer. Improved green fluorescent protein by molecular evolution using DNA shuffling. *Nature Biotechnology*, 14(3), 1996.

[62] Roger Heim, Douglas C. Prasher, and Roger Y Tsien. Wavelength mutations and posttranslational autoxidation of green fluorescent protein. *Proceedings of the National Academy of Sciences of the United States of America*, 91(26):12501–12504, 1994.

[63] Andrea Sacchetti, Valeria Cappetti, Pierfrancesco Marra, Roberta Dell'Arciprete, Tarek El Sewedy, Carlo Crescenzi, and Saverio Alberti. Green fluorescent protein variants fold differentially in prokaryotic and eukaryotic cells. *Journal of Cellular Biochemistry*, 81(S36):117–128, 2001.

[64] Bo Shui, Abdullah Ozer, Warren Zipfel, Nevedita Sahu, Avtar Singh, John T Lis, Hua Shi, and Michael I Kotlikoff. RNA aptamers that functionally interact with green fluorescent protein and its derivatives. *Nucleic Acids Research*, 40(5), 2012.

[65] Joanna Krasowska, Monika Olasek, Agnieszka Bzowska, Patricia L Clark, and Beata Wielgus-Kutrowska. The comparison of aggregation and folding of enhanced green fluorescent protein (EGFP) by spectroscopic studies. *Spectroscopy*, 24(3-4):343–348, 2010.

[66] Richard N. Day and Michael W. Davidson. The fluorescent protein palette: Tools for cellular imaging. *Chemical Society Reviews*, 38(10):2887–2921, 2009.

[67] Valerie L. Anderson and Watt W. Webb. A desolvation model for trifluoroethanol-induced aggregation of enhanced green fluorescent protein. *Biophysical Journal*, 102(4):897–906, 2012.

[68] Wei Wang and Christopher J. Roberts. Protein aggregation – Mechanisms, detection, and control, 2018.

[69] Wei Wang, Sandeep Nema, and Dirk Teagarden. Protein aggregation-Pathways and influencing factors, 2010.

[70] Brock C Roughton, Lavanya K Iyer, Esben Bertelsen, Elizabeth M Topp, and Kyle V Camarda. Protein aggregation and lyophilization: Protein structural descriptors as predictors of aggregation propensity. *Computers and Chemical Engineering*, 58:369–377, 2013.

[71] `http://n2t.net/addgene:54762`.